

## **A polygenic and phenotypic risk prediction for Polycystic Ovary Syndrome evaluated by Phenome-wide association studies**

Short title: PRS & PheWAS of PCOS in 124,852 adults from electronic health records

Yoonjung Yoonie Joo<sup>1</sup>, Ky'era Actkins<sup>2</sup>, Jennifer A. Pacheco<sup>3</sup>, Anna O. Basile<sup>4</sup>, Robert Carroll<sup>5</sup>, David R. Crosslin<sup>6</sup>, Felix Day<sup>7</sup>, Joshua C. Denny<sup>5</sup>, Digna R. Velez Edwards<sup>5,8</sup>, Hakon Hakonarson<sup>9,10</sup>, John B. Harley<sup>11,12</sup>, Scott J Hebring<sup>13</sup>, Kevin Ho<sup>14</sup>, Gail P. Jarvik<sup>15</sup>, Michelle Jones<sup>16</sup>, Tugce Karderli<sup>17</sup>, Frank D. Mentch<sup>9</sup>, Cindy Meun<sup>18</sup>, Bahram Namjou<sup>11</sup>, Sarah Pendergrass<sup>14</sup>, Marylyn D. Ritchie<sup>19</sup>, Ian B. Stanaway<sup>6</sup>, Margrit Urbanek<sup>1</sup>, Theresa L. Walunas<sup>20</sup>, Maureen Smith<sup>3</sup>, Rex L. Chisholm<sup>3</sup>, International PCOS Consortium, Abel N. Kho<sup>20</sup>, Lea Davis<sup>5</sup>, M. Geoffrey Hayes<sup>1,3,21</sup>

1. Division of Endocrinology, Metabolism, and Molecular Medicine, Department of Medicine, Northwestern University Feinberg School of Medicine, Chicago, IL, 60611, USA
2. Department of Microbiology, Immunology, and Physiology, Meharry Medical College, Nashville, TN, 37203, USA
3. Center for Genetic Medicine, Northwestern University Feinberg School of Medicine, Chicago, IL, 60611, USA
4. Department of Biomedical Informatics, Columbia University New York, NY, 10032, USA
5. Departments of Biomedical Informatics and Medicine, Vanderbilt University Medical Center, Nashville, TN, 37203, USA
6. Department of Biomedical Informatics and Medical Education, University of Washington School of Medicine, Seattle, WA, 98195, USA
7. MRC Epidemiology Unit, Cambridge Biomedical Campus, University of Cambridge School of Clinical Medicine, Cambridge, CB2 0QQ, United Kingdom
8. Division of Quantitative Sciences, Department of Obstetrics and Gynecology, Vanderbilt University Medical Center, Nashville, TN, 37203, USA
9. Center for Applied Genomics, Children's Hospital of Philadelphia, Philadelphia, PA, 19104, USA

10. Department of Pediatrics, The Perelman School of Medicine, University of Pennsylvania, Philadelphia, PA, 19104, USA
11. Center for Autoimmune Genomics and Etiology (CAGE), Cincinnati Children's Hospital Medical Center, Cincinnati, OH 45229, USA
12. Department of Pediatrics, University of Cincinnati College of Medicine; US Department of Veterans Affairs, Cincinnati, OH 45229, USA
13. Center for Precision Medicine Research, Marshfield Clinic Research Institute, Marshfield, WI, 54449, USA
14. Biomedical and Translational Informatics, Geisinger, Danville, PA, 17822, USA
15. Division of Medical Genetics, Department of Medicine (Medical Genetics) and Genome Sciences, University of Washington Medical School, Seattle, WA, 98195, USA
16. Center for Bioinformatics & Functional Genomics, Department of Biomedical Sciences, Cedars-Sinai Medical Center, Los Angeles, CA, 90048, USA
17. The Wellcome Trust Centre for Human Genetics, University of Oxford, Oxford, OX3 7BN, United Kingdom
18. Department of Obstetrics and Gynecology, Erasmus MC, University Medical Center Rotterdam, Rotterdam, The Netherlands
19. Department of Genetics, University of Pennsylvania, Philadelphia, PA, 19104, USA
20. Division of General Internal Medicine and Geriatrics, Department of Medicine, Northwestern University Feinberg School of Medicine, Chicago, IL, 60611, USA
21. Department of Anthropology, Northwestern University, Evanston, IL 60208, USA

## **Keywords**

Phenome-wide association study, Genomic prediction, Polygenic risk score, Polycystic Ovary Syndrome

## **Abstract (~300 words)**

### **Purpose**

As many as 75% of patients with Polycystic ovary syndrome (PCOS) are estimated to be unidentified in clinical practice. Utilizing polygenic risk prediction, we aim to identify the phenome-wide comorbidity patterns characteristic of PCOS to improve accurate diagnosis and preventive treatment.

### **Methods and Findings**

Leveraging the electronic health records (EHRs) of 124,852 individuals, we developed a PCOS risk prediction algorithm by combining polygenic risk scores (PRS) with PCOS component phenotypes into a polygenic and phenotypic risk score (PPRS). We evaluated its predictive capability across different ancestries and perform a PRS-based phenome-wide association study (PheWAS) to assess the phenomic expression of the heightened risk of PCOS. The integrated polygenic prediction improved the average performance (pseudo- $R^2$ ) for PCOS detection by 0.228 (61.5-fold), 0.224 (58.8-fold), 0.211 (57.0-fold) over the null model across European, African, and multi-ancestry participants respectively. The subsequent PRS-powered PheWAS identified a high level of shared biology between PCOS and a range of metabolic and endocrine outcomes, especially with obesity and diabetes: 'morbid obesity', 'type 2 diabetes', 'hypercholesterolemia', 'disorders of lipid metabolism', 'hypertension' and 'sleep apnea' reaching phenome-wide significance.

### **Conclusions**

Our study has expanded the methodological utility of PRS in patient stratification and risk prediction, especially in a multifactorial condition like PCOS, across different

genetic origins. By utilizing the individual genome-phenome data available from the EHR, our approach also demonstrates that polygenic prediction by PRS can provide valuable opportunities to discover the pleiotropic phenomic network associated with PCOS pathogenesis.

## 1 Introduction

2

3 Polycystic ovary syndrome (PCOS) is the most common reproductive metabolic  
4 disorders, affecting 5-15% of reproductive age women worldwide [1]. The estimated  
5 cost of diagnosing and treating American women with PCOS is \$5.46 billion annually as  
6 of 2017 [2, 3]. In addition to being a major cause of female infertility, the disease is a  
7 well-known risk factor for endocrine complications, such as type 2 diabetes, impaired  
8 glucose tolerance, and metabolic syndrome before age 40 [4]. Monozygotic twin studies  
9 of PCOS have suggested that PCOS is highly heritable ( $h^2 = \sim 70\%$ ) [5] and the genetic  
10 architecture is polygenic with complex genetic inheritance pattern [6, 7]. Despite its  
11 clinical importance and high heritability, the underlying genetic etiology of PCOS  
12 remains incompletely understood. The phenotypic manifestations of PCOS are  
13 heterogeneous and exhibit considerable variation across race and ethnicity, further  
14 complicating the clinical diagnosis. Currently, it is estimated that up to 75% of women  
15 with PCOS remain undiagnosed in part due to varying diagnostic criteria from the  
16 National Institutes of Health (NIH), Rotterdam, or Androgen Excess Society, [8-12]  
17 which use different combinations of hyperandrogenism, ovulatory dysfunction, and/or  
18 polycystic ovarian morphology. Despite shared genetic risk across the criteria [13], the  
19 disagreement regarding PCOS phenotypic criteria presents a significant challenge for  
20 both clinical practice and research [14, 15]. The commonalities and differences between  
21 the phenotypic characteristics of PCOS may be better understood with an integrative  
22 observation of phenome-wide pleiotropies and co-morbidities.

23 Polygenic risk scores (PRS) built from well-powered genome-wide association  
24 studies (GWAS) have demonstrated operationalizing potential as biological risk  
25 predictors for patient stratification and risk prediction [16-19]. PRS represents the  
26 cumulative effect of common genetic variation summed per individual into a single risk  
27 score, providing an intuitive way to translate GWAS findings into clinically relevant  
28 information such as a patient's risk of disease [20, 21]. From a precision medicine  
29 perspective, PRS hold significant promise especially for a multifactorial condition with  
30 complicated clinical manifestations, such as PCOS. However, several practical  
31 challenges remain in the equitable translation of PRS into clinical practice [22, 23]. For  
32 instance, most GWAS have been performed in samples of primarily European ancestry,  
33 resulting in PRS statistics that systematically perform worse in populations of different  
34 ancestry, including African ancestry populations. This underperformance is due to a  
35 combination of population-specific genetic effects that are undetected in a Euro-centric  
36 GWAS, and differences in the patterns of linkage disequilibrium (LD) between  
37 populations of differing biogeographic ancestry [24-27]. Thus, the evaluation of PRS  
38 from existing GWAS in both European and non-European ancestry samples is a critical  
39 step in setting priorities for equitable precision medicine initiatives.

40 The widespread deployment of Electronic Health Records (EHRs) and the  
41 availability of these multi-dimensional records enables evaluation of PRS in a research  
42 context that mimics a clinical hospital setting. Using these data, the predictive capability  
43 of PRS can be assessed regarding many possible diagnoses that can accumulate  
44 during an individual's lifespan (i.e., the phenome). The eMERGE (electronic MEDical  
45 Records and GENomics) Network is a nationwide consortium of multiple medical

46 institutions that link DNA biobanks to EHRs [28], which is an important resource for  
47 determining the clinical utility of genomic findings, and enabling exploration of the range  
48 of phenotypes associated with genetic variation [29, 30].

49 The aim of this study is to systematically examine the utility of PRS derived from a  
50 GWAS meta-analysis by the International PCOS Consortium [13] for risk prediction  
51 across multiple ancestries and to further characterize the other EHR phenotypes that  
52 are clinically associated with PCOS genetic risk in both women and men. We first  
53 developed the integrative polygenic and phenotypic risk score (PPRS) for PCOS by  
54 combining the patient DNA genotype information and PCOS phenotypic elements from  
55 the EHR. Then we tested the predictive utility of the algorithm within European ancestry  
56 (EA) samples and further evaluated its performance in African ancestry (AA) and  
57 combined multi-ancestry (MA) participants which included EA, AA, and other ancestries.  
58 In addition, we performed a Phenome-Wide Association Study (PheWAS) of the PPRS  
59 for PCOS to identify the range of phenotypic indicators associated with PCOS and  
60 evaluated the predictive characteristics of PPRS to identify underlying PCOS  
61 pathophysiological pathways.

62

63

64

65

66

67

## 68 **Materials and Methods**

### 69 ***PCOS Polygenic Risk Score (PRS) Development***

70 We obtained the full summary statistics of the largest meta-GWAS of PCOS through  
71 the International PCOS consortium and developed a PRS for PCOS [13].

72 **(Supplementary table 1)** The GWAS was conducted in 5,209 cases and 32,055  
73 controls of EA women who were diagnosed according to either NIH or Rotterdam  
74 criteria. All variant positions were converted to GrCh37 and we excluded any entries  
75 with missing ORs or risk allele frequency (RAF) information. The RAF of each variant  
76 was calculated using PLINK [31], and we excluded the entries which RAF deviates  
77 more than 15% than our eMERGE data in order to ensure additional quality control  
78 (QC). PRSice software [32] was used to filter any correlated SNVs in pairwise Linkage  
79 Disequilibrium (LD) ( $r^2 > 0.2$ ) and constructed PRS for PCOS by summing the best-  
80 guess imputed genotype data of PCOS risk variants in each individual weighted by the  
81 reported effect sizes. We used eight different subsets of PCOS susceptibility SNVs to  
82 build the model based on p-value cutoff and compared for their predictive accuracy in  
83 the following validation step:  $5 \times 10^{-8}$ ,  $5 \times 10^{-7}$ ,  $5 \times 10^{-6}$ ,  $5 \times 10^{-5}$ ,  $5 \times 10^{-4}$ ,  $5 \times 10^{-3}$ ,  $5 \times 10^{-2}$ , and  
84 1 (All SNVs).

85

### 86 ***PRS/PPRS Evaluation & PheWAS Discovery Cohort***

87 Our cohort included genotypes and clinical diagnosis records of 99,185 individuals  
88 collected from 12 EHR-linked biobanks nationwide through the eMERGE consortium  
89 [29]. After identity-by-descent (IBD) analysis, we removed 8,019 related individuals that



90 were not in canonical IBD position or genetically identical individuals near the origins  
91 ( $Z_0 > 0.83$  and  $Z_1 < 0.1$ ). The cohort was composed of multiple self-reported and 3<sup>rd</sup>  
92 party observed ancestries and we defined them into three main genetic ancestral  
93 groups using the intersection of self-reported ancestries and principal component  
94 analysis (PCA) based k-mean clusters: European (71.7%), African (15.0%), and Asian  
95 (1.0%). We excluded any self-reported or genetically Hispanic participants for ancestry-  
96 stratified analysis for better homogeneity. Throughout this study, the first four principal  
97 components (PCs) were used to correct population structure, explaining over 17% of  
98 the variances among different genetic origins.

99 The phenome data of the participants were collected from the EHR including  
100 diagnostic records and basic demographic information. The data collection was  
101 performed under local institutional review board approval with informed consent from  
102 the patients. Diagnostic information was structured in the format of the International  
103 Classification of Diseases, Clinical Modification (ICD-CM) codes, in both 9th and 10th  
104 edition, and aggregated into a higher level of 1,711 phecodes for a standardized  
105 categorical analysis of diseases (Phecode map version 1.2) [33, 34]. We excluded 23  
106 individuals under the age of 14, the clinically plausible age for PCOS diagnosis, which is  
107 defined as two years after the first menstruation. A demographic information of the  
108 91,144 participants after filtering criteria is presented in **Table 1**.

109

### 110 ***Genotype data and Quality Control***

111 The participants provided their saliva samples for genotyping, which were  
112 genotyped on 78 genotype Illumina or Affymetrix array batches from 12 medical sites.

Table 1: Demographic and clinical characteristics of discovery cohorts (eMERGE) and replication cohort (BioVU).

Site*	N Subjects	Sex (Female)	Ancestry (EA)	Ancestry (AA)	Age Average	Age SD	BMI Average	BMI SD	PCOS cases	Hirsutism cases	Irregular Mense cases	Female Infertility cases
<b>BSCH**</b>	862	362 (42.2%)	623	74	N/A	N/A	N/A	N/A	2	5	20	0
<b>CCHMC**</b>	5385	2320 (43.2%)	4058	523	8.9	6.7	20.9	6.2	11	24	54	2
<b>CHOP**</b>	9528	4376 (46.0%)	4898	4105	9.8	5.3	21.1	6.2	47	39	205	2
<b>Columbia</b>	2029	989 (48.8%)	519	143	56.1	19.8	27.0	5.4	3	4	15	1
<b>Geisinger</b>	2785	1320 (47.5%)	2439	8	62.8	15.7	32.6	8.1	77	48	158	8
<b>Harvard</b>	23922	13135 (55.0%)	20727	1343	55.3	16.5	28.3	5.8	417	322	2284	217
<b>KPW/UW</b>	3225	1829 (56.7%)	2891	109	76.1	8.9	26.4	4.8	2	25	10	18
<b>Mayo Clinic</b>	9307	4672 (50.2%)	6680	17	61.7	15.4	29.3	5.8	48	85	217	17
<b>Marshfield</b>	3725	2255 (60.9%)	3696	2	69.3	11.0	29.6	6.0	6	84	476	43
<b>Mt. Sinai</b>	5765	3362 (58.8%)	702	3643	59.6	10.0	30.6	7.4	51	45	200	15
<b>Northwestern</b>	4719	3913 (82.9%)	2250	301	53.7	14.8	28.7	7.2	65	83	280	51
<b>Vanderbilt***</b>	19892	10810 (54.4%)	15902	3371	56.6	17.1	29.4	7.1	220	144	1017	48
<b>All (Discovery Cohort)</b>	91144	49343	65385	13639	.	.	.	.	949	908	4936	422

	N Subjects	Sex (Female)	Ancestry (EA)	Ancestry (AA)	Age Average	Age SD	BMI Average	BMI SD	PCOS cases	Hirsutism cases	Irregular Mense cases	Female Infertility cases
<b>VUMC Replication Sample (BioVU)</b>	33708	18096 (54%)	33708	N/A	55.7	20	28.2	6.8	284	225	4330	48

\* BSCH = Boston Children's Hospital, CCHMC=Cincinnati Children's Hospital Medical Center, CHOP= Children's Hospital of Philadelphia, KPW/UW = Group Health Cooperative/University of Washington

\*\* Children's hospital with low average age

\*\*\* No Sample Overlap with replication cohort (BioVU)

113 We used the Michigan Imputation Server(MIS) [35] with the minimac3 missing genotype  
114 variant imputation algorithm to impute missing genotypes in our sample based on the  
115 Haplotype Reference Consortium (HRC1.1) which includes ~65,000 individuals of  
116 diverse ancestry [36]. The imputation resulted in a genome-wide set of ~40 million  
117 SNVs. We filtered the poorly imputed genetic variants with the r-squared imputation  
118 quality threshold (mean variant r-square) less than 0.3, minor allele frequency (MAF)  
119 less than 0.05 and genotype call rate lower than 95%, which resulted in 5,760,270  
120 autosomal polymorphic variants for subsequent analysis. The detailed data collection  
121 and QC report for the eMERGE network is reported elsewhere [29].

122

### 123 ***Validation of Polygenic Risk Score***

#### 124 *A. Predictive ability of each prediction model with different PRS*

125 We performed logistic regression analysis to demonstrate the prediction ability of  
126 PRS for PCOS diagnosis in the female population of three different genetic racial  
127 cohorts: European (n=33,869), African (n=8,198), and the entire admixed cohort  
128 (n=49,365). Each cohort was randomly divided into 75% training and 25% testing set to  
129 separately calculate the regression statistics and out-of-sample prediction error. Using  
130 generalized linear model, the residuals of PRS after covariate adjustments (first four  
131 PCs, sites) were obtained and scaled to build the logistic regression model in the  
132 training set. Regression coefficients and p-value of PRS variable, and pseudo-R<sup>2</sup> of the  
133 eight different PRS models were measured.

134 We applied the regression model built out of the training set to measure out-of-  
135 sample performance in the testing dataset. We predicted the individuals as ‘PCOS  
136 cases’ if their fitted scores are higher than the average fitted score and calculated the  
137 accuracy by comparing with their actual diagnosis records of PCOS. The overall  
138 accuracy, sensitivity, specificity of each model were measured and structured through  
139 confusion matrix. The area under the receiving operating characteristic (ROC) curve,  
140 AUC, was also measured for classifier performance of each model.

#### 141 *B. Stratification ability of each prediction model with different PRS*

142 To evaluate the phenotypic stratification ability of PRS, we divided the cohort into  
143 ten quantiles based on PRS of each individual and compared the average phenotypic  
144 values (e.g. proportion of PCOS diagnosed patients, body mass index (BMI), PRS)  
145 among the groups. The proportion of PCOS patients in each quantile, average PRS  
146 values, and average BMI measures of each individual were analyzed. We also  
147 performed independent t-test to assess if the average PRS score differences between  
148 PCOS cases and controls were statistically significant.

#### 149 *C. Performance improvement by the PRS variable*

150 To estimate the performance of the PRS variable, we built a null regression model  
151 without the PRS variable for PCOS prediction (PRS model vs. Null model). The  
152 incremental pseudo- $R^2$  by McFadden’s [37] were calculated between the PRS models  
153 and the null logistic regression only with first 4 PCs and site variables. The analysis of  
154 variance (ANOVA) was performed to examine how significant PRS variable impacts the  
155 PCOS diagnosis prediction model compared to the null model.

156

157 PRS model:

$$158 \quad \text{logit}(\text{PCOS diagnosis} = 1) = \beta_0 * \mathbf{PRS} + \beta_1 * \text{Site} + \beta_2 * 4\text{PCs} + \beta_3$$

159 Null model:

$$160 \quad \text{logit}(\text{PCOS diagnosis} = 1) = \beta_0 * \text{Site} + \beta_1 * 4\text{PCs} + \beta_2$$

161

## 162 ***Development of prediction algorithms with PRS and PCOS component***

### 163 ***phenotypes (PPRS)***

164 We built an integrative polygenic and phenotypic risk score (PPRS) with PRS and  
165 PCOS component phenotypes in the EHR to maximize the utility of PRS for risk  
166 prediction. Additional dichotomous phenotypic variables to each individual from their  
167 EHR diagnosis records: hirsutism (ICD9 code 704.1, ICD10 code L68.0), irregular  
168 menstruation (ICD9 code 626.4, ICD10 code N92.6), and female infertility (ICD9 code  
169 627, ICD10 code N97.0) were selected, all of which are well-established clinical  
170 components of PCOS. A total 908 individuals with hirsutism, 4,936 individuals with  
171 irregular menstruation, and 422 individuals with female infertility ICD diagnosis codes  
172 were identified in the eMERGE consortium database.

173 Firstly, the logistic regression adjusted for first four PCs and sites were examined  
174 for their effect coefficients and variable p-values. Psuedo-R<sup>2</sup> of each model was  
175 calculated for measuring the improvement over the normal PRS model. ANOVA  
176 between the integrative model and normal PRS model were examined.

177

178 PPRS model:

$$\begin{aligned} 179 \quad \text{logit}(\text{PCOS diagnosis} = 1) &= \beta_0 * \mathbf{PRS} + \beta_1 * \mathbf{Site} + \beta_2 * \mathbf{4PCs} + \beta_3 * \mathbf{Hirsutism} \\ 180 \quad &+ \beta_4 * \mathbf{Irregular menstruation} + \beta_5 * \mathbf{Female infertility} + \beta_6 \end{aligned}$$

181 PPRS null model:

$$\begin{aligned} 182 \quad \text{logit}(\text{PCOS diagnosis} = 1) &= \beta_0 * \mathbf{Site} + \beta_1 * \mathbf{4PCs} + \beta_2 * \mathbf{Hirsutism} + \\ 183 \quad &\beta_3 * \mathbf{Irregular menstruation} + \beta_4 * \mathbf{Female infertility} + \beta_5 \end{aligned}$$

184

### 185 ***Phenome-wide analysis***

186 To investigate the potential pleiotropy of PCOS, PCOS components, and other  
187 diseases in the EMR phenome, we selected the best performing PRS model that  
188 presented a validated predictive accuracy and stratification ability across ancestries  
189 based on the examination results above. PheWAS was performed on the mapped 1,711  
190 representative EHR phenotypes with a minimum of 30 case patients from the discovery  
191 cohort of 91,144 participants after QC criteria. Case group for a given phecode is  
192 defined by the presence of at least one assignment of the corresponding ICD codes  
193 from EHR as defined in the phecode map v1.2. Controls for each phecode are defined  
194 by the absence of the same ICD codes that defined cases and the absence of clinically  
195 related phenotypes. Based on the assumption that a participant with higher PCOS-PRS  
196 conveys greater genetic risk, our main sex-stratified PheWAS interrogated the comorbid  
197 networks of high-risk predictive phenotypes for PCOS (**PheWAS-1**). 49,343 female  
198 participants and 41,669 male participants were used for the analysis. Logistic

199 regression was used adjusting for genotyping site and the first four PCs of ancestry to  
200 correct for population stratification in the MA cohort [ $\text{logit}(\text{Clinical Phenotype} = 1 | \text{PRS},$   
201  $\text{Site}, 4\text{PCs}) = \beta_0 + \beta_1 * \text{PRS} + \beta_2 * \text{Site} + \beta_3 * 4\text{PCs}$ ].

202 In this study, phenome-wide significance refers to either (1) the Bonferroni corrected  
203 threshold of  $p\text{-value} = 2.9 \times 10^{-5}$  adjusting for multiple testing, which is determined by  
204 using the  $p\text{-value}$  of 0.05 divided by the 1,711 phenotypes interrogated, or (2) the false  
205 discovery rate (FDR) significance of 0.05, which is a popular alternative threshold to the  
206 stringent Bonferroni correction in reporting PheWAS. Manhattan PheWAS plots of -  
207  $\log_{10}(p\text{-value})$  were generated for visual inspection of significant clinical traits. All the  
208 analyses were performed in the R statistical software environment (ver 2.1.2).

209

## 210 **Sensitivity Analysis**

211 We performed several comparative PheWAS in an effort to interrogate different  
212 phenome-wide aspects of the PRS in clinical phenome.

213 Firstly, to distinguish secondary or symptomatic phenotypes derived from the  
214 PCOS-diagnosed patients, we removed the clinical diagnosis records of the 949  
215 individuals with PCOS (phecode 256.4, ICD9 256.4 and ICD10 E28.2) and performed  
216 the same PheWAS analysis. **(PheWAS-2)**. Additionally, to gauge the contrasting  
217 performance of polygenic prediction over a single-variant approach, we performed  
218 traditional PheWAS of each genome-wide significant susceptibility loci ( $p\text{-value} < 5 \times 10^{-8}$ )  
219 for PCOS (RAF > 0.05). This analysis aims to compare the clinical phenotypes  
220 associated with the cumulative effects of multiple genetic variants on PRS versus a

221 single genetic signal generated by an individual PCOS susceptibility locus. Among 113  
222 genome-wide significant loci ( $p$ -value  $< 5 \times 10^{-8}$ ) for PCOS, (**Supplementary Table 1**) we  
223 filtered the entries with MAF  $> 0.05$  and genotype call rate  $> 0.90$  in our discovery  
224 cohort and MAF  $> 0.01$  in summary statistics. 85 SNVs were selected and used for the  
225 subsequent PheWAS analysis (**PheWAS-3**).

226

### 227 ***PRS PheWAS Replication***

228 To confirm the predictive performance of our PRS algorithm and its effect on clinical  
229 phenome, replication analyses were performed at Vanderbilt University Medical Center  
230 on an independent genotyped sample of 33,708 European descent individuals (BioVU).  
231 The participants were genotyped on the Illumina MEGAEX platform (~2 million markers)  
232 and we applied filters for individual call rates  $< 98\%$ , batch effects ( $p$ -value  $< 5 \times 10^{-5}$ ),  
233 heterozygosity ( $|F_{het}| > 0.2$ ), and sample relatedness ( $\rho_{ihat} > 0.2$ ). After imputation with  
234 1000G reference panel, we excluded any genetic variants with missingness  $> 0.02$ ,  
235 certainty  $< 0.9$ , or imputation info score  $< 0.95$ . The genetic ancestry of the samples  
236 were restricted to only EA, based on comparison to 1000G European population and a  
237 K-means clustering definition. The final samples included 33,708 individuals of  
238 European descent genotyped on 5,550,390 SNVs. Using the same PRS generation  
239 methodology in discovery samples, we took the identical phenome-wide approach to  
240 identify the associated phenotypic networks with PRS among the replication samples.  
241 Logistic regression was used adjusting for first four ancestry PCs.

### 242 **Results**



243 ***Polygenic risk scores for PCOS are normally distributed in European and multi-***  
244 ***ancestry participants***

245 A total of 5,760,270 autosomal single nucleotide variants (SNVs) were considered  
246 for the PCOS-PRS construction, which displays the genetic architecture of effect size  
247 (beta) by risk allele frequency (RAF) presented in **Figure 1**. There was a significant  
248 negative correlation between RAF and effect size, which is generally anticipated in  
249 common quantitative traits and supports the use of methodology of PRS to explore the  
250 extreme of the common polygenic liability spectrum. According to the central limit  
251 theorem, PRS in a large population will show normality when the genetic architecture of  
252 the target trait is polygenic, i.e. produced by the addition of many genetic variants of  
253 small effect [38, 39].

254 PRS were calculated at eight different p-value cutoffs from the PCOS GWAS  
255 summary statistics ( $5 \times 10^{-8}$ ,  $5 \times 10^{-7}$ ,  $5 \times 10^{-6}$ ,  $5 \times 10^{-5}$ ,  $5 \times 10^{-4}$ ,  $5 \times 10^{-3}$ ,  $5 \times 10^{-2}$ , 1) for all the  
256 discovery eMERGE participants (n=91,144). Each set of scores were adjusted for  
257 participant site and first four PCs. All the polygenic scores were evaluated for their  
258 predictive performance in the female populations of EA (n=33,869), AA (n=8,198) and  
259 MA cohorts (n=49,365). The covariate-adjusted PCOS-PRS generally presented a  
260 normal distribution across each ancestry cohort (**Supplementary Figure 1**). PRS  
261 models with trimodal or skewed distributions (PRS p-value cutoff:  $5 \times 10^{-7}$ ,  $5 \times 10^{-6}$ ,  $5 \times 10^{-5}$ ),  
262 which may be a function of poor representation of risk variants across populations,  
263 were not considered for the subsequent phenome-wide analysis.

264

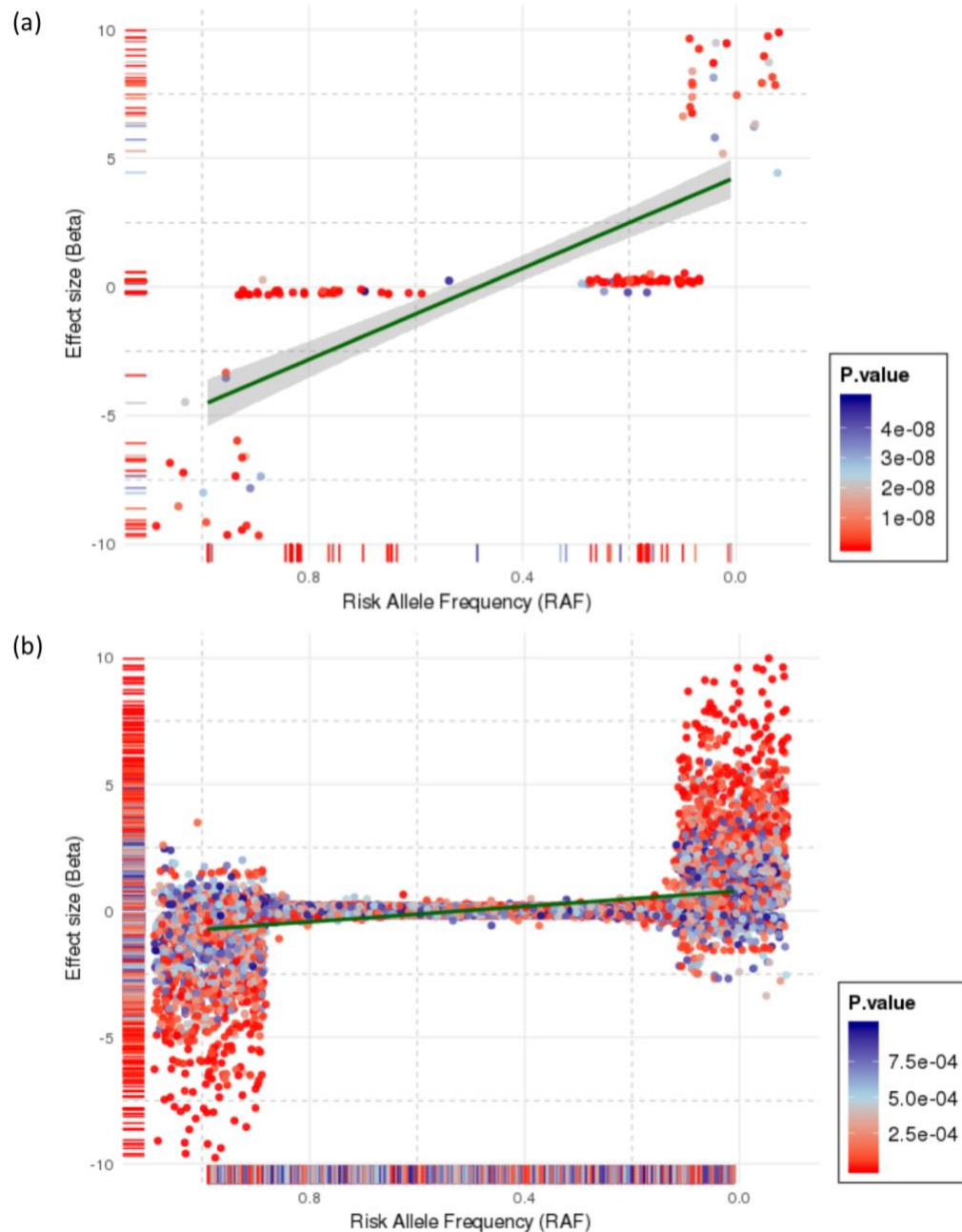


**Fig 1. Effect distribution of PCOS susceptibility variants in samples from the International PCOS consortium by risk allele frequency. (a)** The 120,340 PCOS autosomal SNVs with p-value < 0.05, and **(b)** the 139 PCOS genome-wide significant SNVs (p-value < 5×10<sup>-8</sup>). The dark green line and grey band around it are the linear regression fit and its 95% confidence interval, respectively, between risk allele frequency and effect size (beta).

266 *A. Predictive ability of each prediction model with different PRS*

267 In the PRS prediction models using the training set of the female EA cohort  
268 (n=33,869 with 632 PCOS cases), all the coefficient p-values of the PRS variables are  
269 statistically significant except for two PRS models of SNVs with p-value  $< 5 \times 10^{-7}$  and p-  
270 value  $< 5 \times 10^{-6}$  that do not show PRS normality (**Supplementary Figure 1**). The  
271 average odds ratios (OR) of the significant PRS variable across EA was 1.13 (average  
272 SE=0.046) and the average pseudo-R<sup>2</sup> value was 0.044, which indicates 4.4% of the  
273 phenotypic variances in the training sample could be explained by PRS (**Table 2**).

274 The regression models built in the training set were then used to predict PCOS case  
275 status in the testing dataset. A model including PRS yielded average prediction  
276 accuracy of 0.55, sensitivity of 0.55, specificity of 0.76 with an average area under the  
277 receiving operating characteristic curve (AUC) of 0.72 in the EA participants (**Table 3**).

278 *B. Stratification ability of each prediction model with different PRS*

279 The percentage of PCOS-diagnosed patients increases in higher PRS quantiles,  
280 and the individuals in the highest PRS group tend to have higher average BMI. In the  
281 genome-wide PRS calculation with SNVs with p-value  $\leq 1$ , the average BMI of the  
282 individuals in highest PRS quantile is 1.1 kg/m<sup>2</sup> higher than the individuals in the lowest  
283 PRS group (Cohen's d=0.16, t-test p-value= $1.06 \times 10^{-9}$ ) (**Figure 2 and Table 4**). The  
284 finding confirms the positive correlation between elevated generic risk for PCOS, actual  
285 PCOS diagnosis, and higher risk for increased BMI.

286

Table 2: Regression results of the PRS and PPRS models in PCOS prediction.

PRS/PPRS p-value Cutoff	PRS*				PPRS*			
	OR	Std. Error	P	R <sup>2</sup>	OR	Std. Error	P	R <sup>2</sup>
<u>European Ancestry</u>								
5E-08	1.14	0.047	4.76E-03	0.045	1.14	0.052	1.40E-02	0.232
5E-07	1.04	0.042	3.78E-01	0.043	1.04	0.046	3.89E-01	0.230
5E-06	1.08	0.039	6.41E-02	0.044	1.08	0.044	7.26E-02	0.231
5E-05	1.10	0.041	2.13E-02	0.044	1.10	0.046	3.59E-02	0.231
5E-04	1.13	0.045	6.12E-03	0.044	1.11	0.049	2.85E-02	0.231
5E-03	1.11	0.047	2.70E-02	0.044	1.08	0.051	1.45E-01	0.231
5E-02	1.16	0.048	2.11E-03	0.045	1.12	0.052	3.21E-02	0.231
1	1.15	0.049	3.13E-03	0.045	1.11	0.052	4.04E-02	0.231
<u>Multiancestry</u>								
5E-08	1.16	0.038	1.15E-04	0.040	1.15	0.042	1.19E-03	0.228
5E-07	1.08	0.037	4.28E-02	0.038	1.09	0.038	2.99E-02	0.227
5E-06	1.09	0.037	1.60E-02	0.038	1.10	0.038	1.19E-02	0.227
5E-05	1.12	0.037	2.35E-03	0.039	1.12	0.038	3.67E-03	0.228
5E-04	1.12	0.038	1.88E-03	0.039	1.11	0.039	8.59E-03	0.228
5E-03	1.16	0.039	1.25E-04	0.040	1.13	0.041	2.54E-03	0.228
5E-02	1.20	0.039	5.03E-06	0.041	1.16	0.042	3.81E-04	0.228
1	1.22	0.040	5.33E-07	0.041	1.19	0.043	5.91E-05	0.229
<u>African Ancestry</u>								
5E-08	1.14	0.090	1.42E-01	0.031	1.15	0.099	1.62E-01	0.211
5E-07	1.24	0.086	1.22E-02	0.034	1.30	0.093	4.63E-03	0.215
5E-06	1.25	0.086	9.80E-03	0.034	1.30	0.092	3.95E-03	0.216
5E-05	1.23	0.086	1.71E-02	0.034	1.27	0.093	1.08E-02	0.214
5E-04	1.19	0.088	4.38E-02	0.032	1.17	0.094	9.82E-02	0.211
5E-03	1.18	0.090	6.74E-02	0.032	1.18	0.098	9.32E-02	0.211
5E-02	1.25	0.091	1.23E-02	0.034	1.17	0.097	1.07E-01	0.211
1	1.30	0.091	3.33E-03	0.036	1.26	0.097	1.56E-02	0.214

**Average of the significant models (regression coefficient p-value < 0.05)**

PRS	Average OR	Average R <sup>2</sup>	Null R <sup>2</sup> **	Incremental R <sup>2</sup> *** over PRS null model
EA	1.13	0.044	0.004	0.041
MA	1.14	0.039	0.004	0.036
AA	1.25	0.034	0.004	0.030

<b>PPRS</b>	<b>Average OR</b>	<b>Average R<sup>2</sup></b>	<b>PPRS Null R<sup>2</sup>**</b>	<b>Incremental R<sup>2</sup>*** over null model</b>	<b>Incremental R<sup>2</sup>*** over PPRS null model</b>
EA	1.12	0.231	0.193	0.228 (61.5-fold)	0.038 (19.6%)
MA	1.13	0.228	0.201	0.224 (58.8-fold)	0.027 (13.2%)
AA	1.28	0.215	0.193	0.211 (57.0-fold)	0.021 (11.0%)

OR = odds ratio; SE = standard error; R<sup>2</sup> = psuedo-R<sup>2</sup>

\* PRS: PRS + basic covariates [Model(1) = PCOS ~ PRS + PC1-4 + Site ]

\* PPRS: PRS + PCOS component phenotypes + basic covariates [PPRS = PCOS ~ PRS + PC1-4 + Site + Hirsutism + Female Infertility + Irregular Menses]

\*\* Null model: basic covariates only [Null Model = PCOS ~ PC1-4 + Site]

\*\* PPRS Null model: PCOS component phenotypes + basic covariates [PPRS Null Model = PCOS ~ PC1-4 + Site + Hirsutism + Female Infertility + Irregular Menses]

\*\*\* Improvement rate: (Incremental change in pseudo-R<sup>2</sup> between the model with PRS/PPRS and the null model without PRS/PPRS) / (Pseudo-R<sup>2</sup> of the null model without PRS/PPRS)

**Table 3:** Average performance of PRS prediction algorithms in the female cohorts of European (n=33,869), Multiancestry (n= 49,365) and African (n=8,198) participants.

**Summary - Average**

<b>PRS*</b>	<b>Accuracy</b>	<b>Sensitivity</b>	<b>Specificity</b>	<b>Balanced Accuracy***</b>	<b>AUC****</b>
<b>European (n=33,869)</b>	0.551	0.547	0.755	0.651	0.715
<b>Multiancestry (n= 49,365)</b>	0.533	0.529	0.736	0.632	0.693
<b>African (n=8,198)</b>	0.496	0.494	0.590	0.542	0.543
<b>PPRS**</b>	<b>Accuracy</b>	<b>Sensitivity</b>	<b>Specificity</b>	<b>Balanced Accuracy***</b>	<b>AUC****</b>
<b>European (n=33,869)</b>	0.873	0.876	0.717	0.797	0.870
<b>Multiancestry (n= 49,365)</b>	0.881	0.886	0.640	0.763	0.823
<b>African (n=8,198)</b>	0.864	0.872	0.522	0.697	0.706

\* PRS: PRS + basic covariates [PRS Model = PCOS ~ PRS + PC14 + Site ]

\*\* PPRS: PRS + PCOS component phenotypes + basic covariates [PPRS Model = PCOS ~ PRS + PC1-4 + Site + Hirsutism + Female Infertility + Irregular Menses]

\*\*\* Balanced Accuracy = (Sensitivity + Specificity)/2

\*\*\*\* AUC = Area Under the Curve

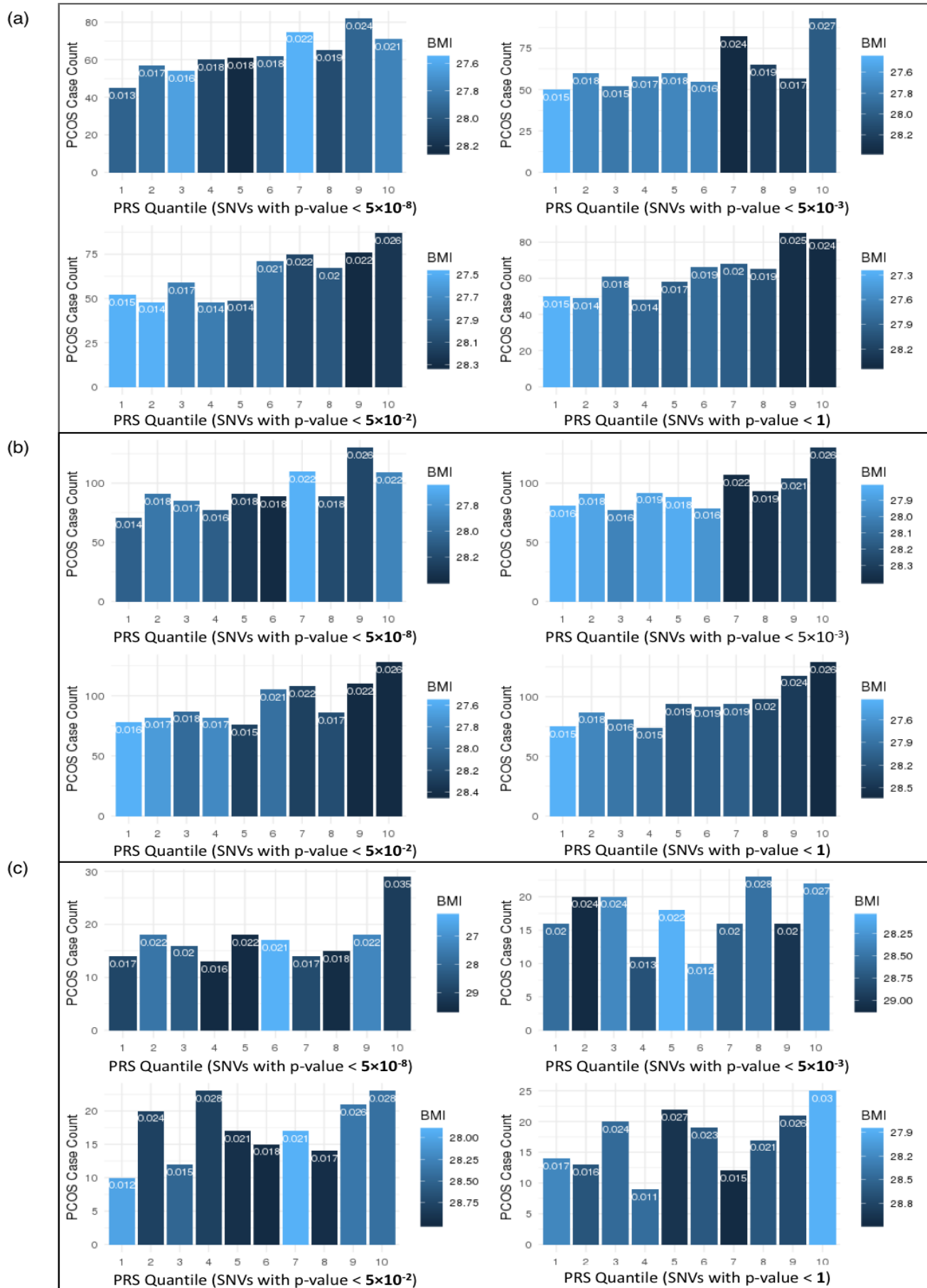


**Fig 2. Stratification performance by quantile of PRS models**, including PCs 1-4 and site as covariates, in (a) EA, (b) MA, and (c) AA populations. Group 1 includes those with the lowest PRS, and group 10 includes those with the highest. Bar colors indicate the average BMI in the quantile (darker indicates higher BMI), while the proportion of PCOS-diagnosed patients in each group is indicated at the top of each bar.



**Table 4:** Quantile analysis of PRS in the female European cohort (n=33,869) (PRS SNVs' p-value $<5 \times 10^{-8}$  and p-value $\leq 1$  only).

	GROUP*	PCOS cases	PCOS prop**	Average BMI (kg/m <sup>2</sup> )	Average PRS
<b>PRS P &lt; 5×10<sup>-8</sup></b>	1	45	1.3%	27.9	-1.750
	2	57	1.7%	27.9	-0.950
	3	54	1.6%	27.6	-0.813
	4	60	1.8%	28.1	-0.239
	5	61	1.8%	28.2	-0.068
	6	62	1.8%	28.0	0.014
	7	75	2.2%	27.6	0.248
	8	65	1.9%	28.1	0.810
	9	82	2.4%	27.9	0.952
	10	71	2.1%	27.8	1.790

...

<b>PRS P ≤ 1</b>	1	50	1.5%	27.3	-1.790
	2	49	1.5%	27.5	-1.020
	3	61	1.8%	27.8	-0.654
	4	48	1.4%	27.9	-0.369
	5	58	1.7%	28.0	-0.113
	6	66	2.0%	27.8	0.132
	7	68	2.0%	28.0	0.386
	8	65	1.9%	28.1	0.672
	9	85	2.5%	28.4	1.040
	10	82	2.4%	28.4	1.720

PRS is adjusted with covariates and scaled for standardization.

\* Higher group number indicates higher PRS

\*\* Proportion of PCOS case patients in the quantile

287 The subsequent t-test reveals that PRS of case patients are significantly higher than  
288 the controls in all the nominally significant PRS models with regression p-value < 0.05,  
289 implying that higher genetic risk scores indicate higher occurrence of PCOS diagnosis  
290 (p-value= $2.15 \times 10^{-4}$ ,  $7.75 \times 10^{-4}$ ,  $2.43 \times 10^{-4}$ ,  $2.51 \times 10^{-5}$ ,  $3.12 \times 10^{-5}$  in PRS model SNVs' p-  
291 value <  $5 \times 10^{-8}$ ,  $5 \times 10^{-4}$ ,  $5 \times 10^{-3}$ ,  $5 \times 10^{-2}$ , 1 respectively) (**Supplementary Table 2**).

### 292 *C. Performance improvement by the PRS variable*

293 All the PRS models containing PCOS-PRS provided an improved fit over the null  
294 model by increasing the estimated explained sum of squares (pseudo- $R^2$ ) by  
295 McFadden's [37]. The average increase of pseudo- $R^2$  by the PRS variable in EA  
296 samples is 0.040, which is a 10-fold improvement ( $=0.040/0.004$ ) over the null model.  
297 The ANOVA p-values of differentiating the PRS models from the null model are all  
298 under  $1 \times 10^{-31}$ , which validate the statistical significance of the performance  
299 improvement over the null model (**Table 2 and Supplementary Table 3**).

300

### 301 ***Evaluation of PRS in multi-ancestry and African ancestry participants***

#### 302 *A. Predictive ability of each prediction model with different PRS*

303 In the training set of the MA cohort (n=49,365 with 949 PCOS cases), the coefficient  
304 p-values of all PRS variables remain significant with positive beta coefficients (**Table 2;**  
305 **model1**). The average OR of PRS is 1.14 (average SE=0.038) and the average  
306 pseudo- $R^2$  value is 0.039, indicating that 3.9% of the phenotypic variance in the MA  
307 cohort could be explained by the PRS model. In the training set of AA participants  
308 (n=8,198 with 172 PCOS cases), the coefficient p-values of PRS variables remain

309 overall significant except for two PRS models of SNVs with p-value  $< 5 \times 10^{-8}$  and p-  
310 value  $< 5 \times 10^{-3}$  which may be due to the smaller sample size. Even though the  
311 regression p-values of the PRS variable do not show uniform performance in AA as  
312 compared to EA, the nominally significant PRS models generate a higher effect size in  
313 the AA samples compared to the other ancestry groups. The average OR of PRS  
314 models in the AA is 1.25 (SE=0.089), higher than both the EA (OR=1.13) and MA  
315 (OR=1.14). This is possibly due to the low RAF of PCOS risk variants in AA compared  
316 to EA (**Supplementary Table 1**).

317 For the testing dataset, PRS prediction displays an average 0.533 of accuracy,  
318 0.529 of sensitivity, 0.736 of specificity with an average AUC of 0.693 in the multi-  
319 ancestry cohort. The out-of-sample performance in AA yielded an average AUC of  
320 0.543 and showed an overall lower average accuracy (0.496), sensitivity (0.494) and  
321 specificity (0.590) compared to other ancestry groups (**Table 3**).

#### 322 *B. Stratification ability of each prediction model with different PRS*

323 In the MA cohort, the proportion of PCOS patients increases from 1.5% in the  
324 lowest quantile to 2.6% in the highest quantile in the PRS calculation of SNVs with p-  
325 value  $\leq 1$ . The average BMI of the participants in the highest PRS quantile is 1.2 kg/m<sup>2</sup>  
326 higher (Cohen's d=0.17, t-test p-value= $1.62 \times 10^{-13}$ ) than the participants in the lowest  
327 PRS group (**Supplementary Table 4, Figure 2(b)**).

328 In the AA cohort, the number of PCOS patients does not always increase with  
329 higher PRS quantile, but the observation of an excess of PCOS patients in the highest  
330 PRS quantile is generally consistent across the models (**Figure 2c**). In the full-inclusive  
331 PRS model (SNVs with p-value  $\leq 1$ ), the rate of PCOS patients increases from 1.7% in

332 the lowest quantile to 3.1% in the highest PRS quantile (**Supplementary table 4**). The  
333 observed increase of the rate of PCOS patients is most pronounced in the PRS model  
334 with genome-wide significant variants (SNVs with p-value  $< 5 \times 10^{-8}$ ), as the PCOS case  
335 rate doubles from 1.7% in the lowest quantile to 3.5% in the highest PRS quantile. We  
336 did not identify any notable trends in BMI in AA participants, which is depicted by the  
337 quantile color changes in **Figure 2(c)**.

338 An independent t-test confirms the significant differences of average PRS between  
339 PCOS cases and controls in MA across the models. The PRS difference between  
340 PCOS MA cases and controls is 0.165 after scaling with a full-inclusive PRS model,  
341 SNVs with p-value  $\leq 1$  (Cohen's  $d=0.201$ , t-test p-value= $2.62 \times 10^{-6}$ ). In AA, only the full-  
342 inclusive PRS model shows statistically significant difference between PCOS cases and  
343 controls with a PRS difference of 0.175 (Cohen's  $d=0.191$ , t-test p-value= $2.90 \times 10^{-2}$ )  
344 (**Supplementary Table 2**).

#### 345 *C. Performance improvement by the PRS variable*

346 In the joint ancestry participants, all the prediction models containing the PRS  
347 variable provide a better fit over the null model by increasing the average pseudo- $R^2$  to  
348 0.039, which is an 8.75-fold increase ( $=0.035/0.004$ ) in explanatory power (**Table 2**).  
349 The subsequent ANOVA analysis confirms the statistical significance of the improved  
350 fits over the null model with all p-values  $< 1 \times 10^{-46}$  (**Supplementary table 3**).

351 In the AA samples, the statistically significant PRS models show the average  
352 pseudo- $R^2$  of 0.034, which has the poorest fit among the ancestries. The models show  
353 an average pseudo- $R^2$  improvement of 7.5-fold increase ( $=0.030/0.004$ ) from the null  
354 model without PRS (**Table 2**). Even with the lowest average incremental pseudo- $R^2$

355 (0.030) among the ancestries, the significant difference between the PRS models and  
356 the null model in Africans are confirmed with all ANOVA p-values $<5\times 10^{-3}$   
357 **(Supplementary table 3).**

358

359 ***Development of PPRS prediction algorithms with PRS and PCOS component***  
360 ***phenotypes***

361 The addition of PCOS component EHR phenotypes to polygenic risk prediction  
362 significantly improved the predictive accuracy **(Table 2; model2 and Figure 3)**. The  
363 average pseudo- $R^2$  of the PPRS is 0.231 in EA, 0.228 in MA, and 0.215 in AA samples,  
364 which indicates an average 14.7% improvement in pseudo- $R^2$  (19.6% in EA, 13.2% in  
365 AA, 11.0% in MA) over the PPRS null model by the inclusion of PCOS component  
366 phenotypes. Compared to the basic null model, the PPRS prediction boosts the average  
367 predictive performance (pseudo- $R^2$ ) by approximately 60 times (61.5-fold in EA, 58.8-  
368 fold in AA, 57.0-fold in MA) by the combinational use of PCOS component EHR  
369 phenotypes and PRS. Of note, the PRS variable's p-values in every PPRS model  
370 remain consistently valid in the MA samples (p-values $<5\times 10^{-3}$ ), whereas it was not  
371 always significant in AA or even EA samples. The ORs of the PRS and PPRS remain  
372 similar across the ancestries **(Figure 4)**.

373 The subsequent ANOVA tested that all the pairs between PPRS and PPRS null  
374 models were statistically distinct across the cohorts and every PPRS model show the  
375 improved fit over the PPRS null model **(Supplementary Table 3)**. The average ORs of  
376 irregular menstruation (ICD9 code 626.4, ICD10 code N92.6), female infertility (ICD9  
377 code 627, ICD10 code N97.0) and hirsutism (ICD9 code 704.1, ICD10 code L68.0) for

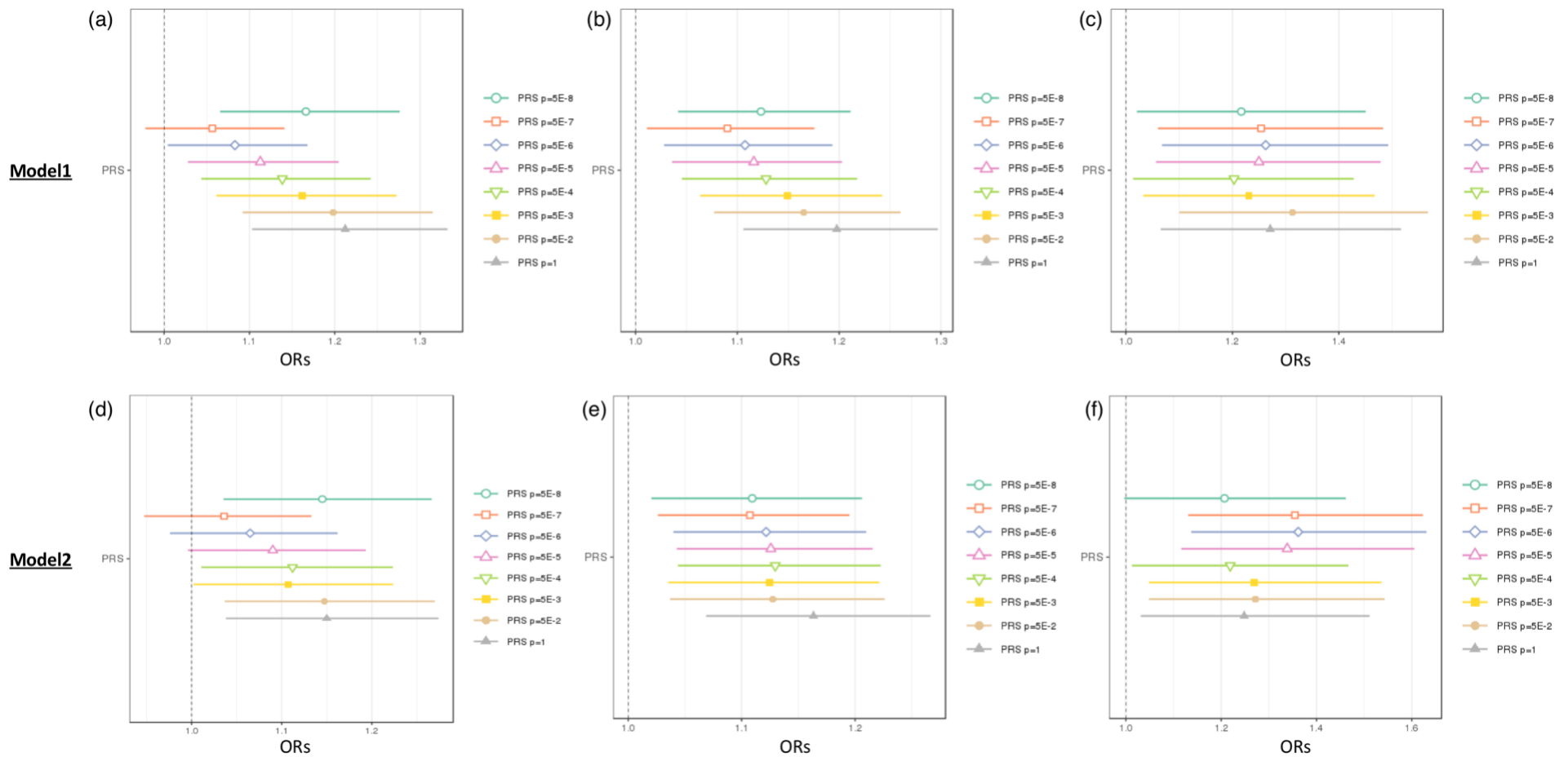
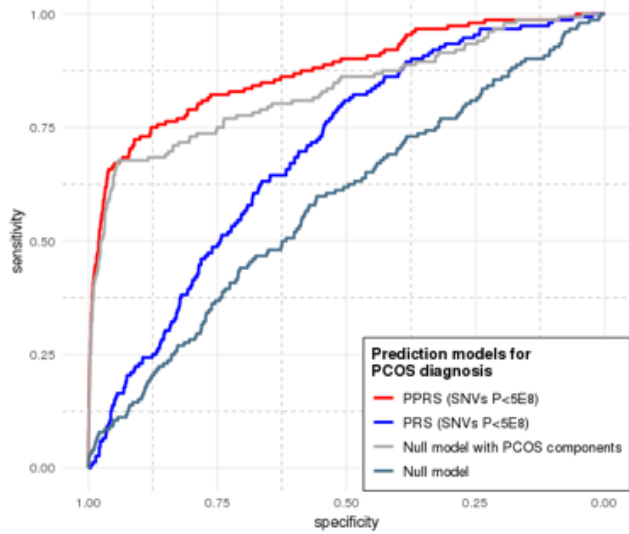
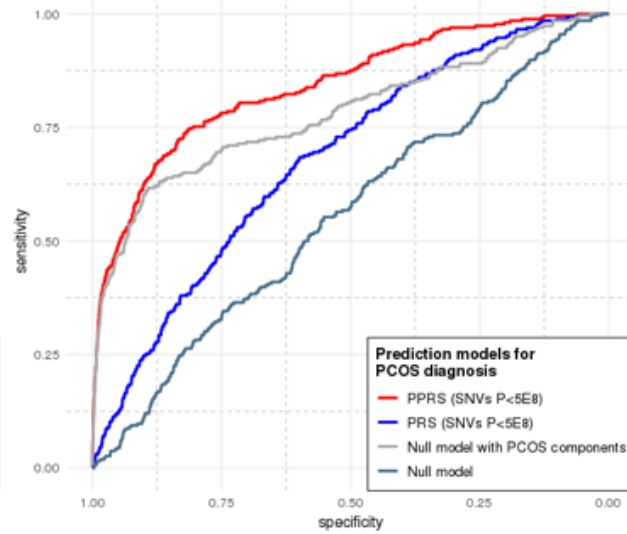


**Figure 3.** Comparison of odds ratios (ORs) for the PRS and PPRS in (a) EA, (b) MA, and (c) AA cohorts, at different PRS/PPRS inclusion thresholds by GWAS p-value. The top row shows OR distributions for the PRS model, which adjusted for basic covariates [PRS Model = PCOS ~ PRS + PC1-4 + Site]. The bottom row shows OR distributions for the PPRS model which adjusted for the same basic covariates as well as PCOS EHR component phenotypes [PPRS Model = PCOS ~ PRS + PC1-4 + Site + Hirsutism + Female Infertility + Irregular Menses].

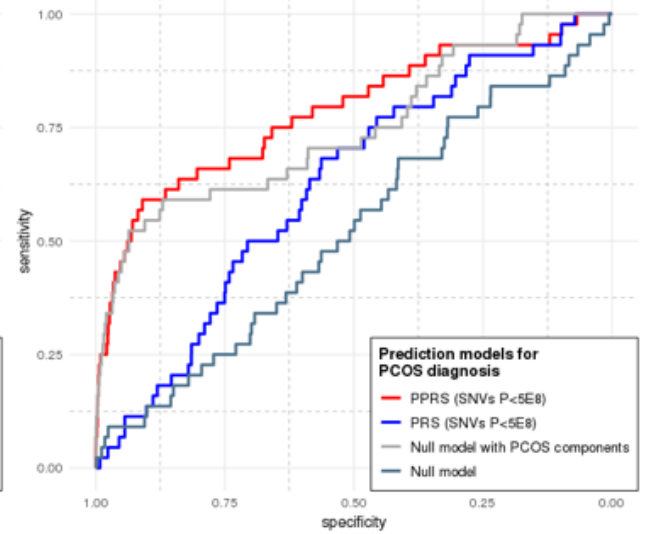
(a) European ancestry (EA)



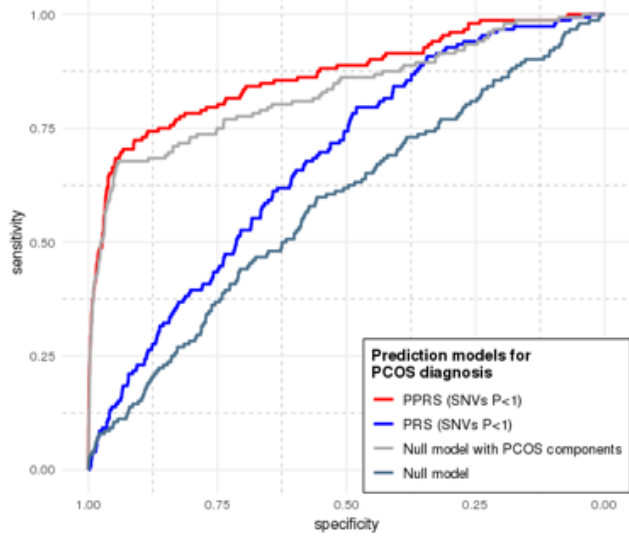
(b) Multiancestry (MA)



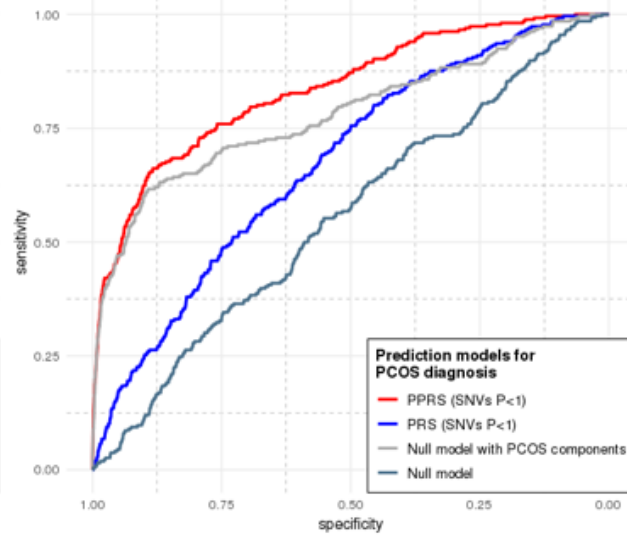
(c) African ancestry (AA)



(d) European ancestry (EA)



(e) Multiancestry(MA)



(f) African ancestry (AA)

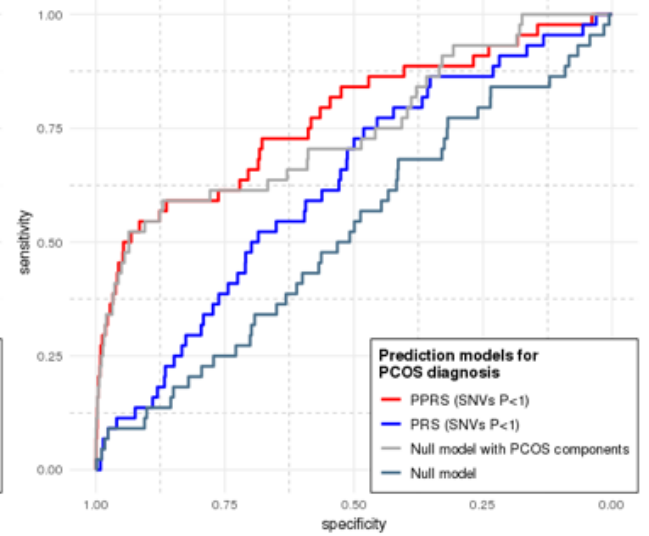


**Figure 4.** Comparison of Receiving Operating Curves (ROC) of the PPRS and PRS prediction models for PCOS diagnosis. The models with the genome-wide significant SNVs ( $p$ -value  $< 5 \times 10^{-8}$ ) were evaluated in females of (a) EA, (b) MA, and (c) AA cohorts, along with the full-inclusive prediction models ( $p$ -value  $< 1$ ) in females of (d) EA, (e) MA, and (f) AA cohorts. The areas under the curve (AUC) are provided in Table 2 and Supplementary Table 2. PRS model adjusted for basic covariates [PRS Model = PCOS ~ PRS + PC1-4 + Site ], and PPRS model adjusted for the same basic covariates as well as PCOS EHR component phenotypes [PPRS Model = PCOS ~ PRS + PC1-4 + Site + Hirsutism + Female Infertility + Irregular Menses]. Null models only included the basic covariates without the PRS variable.



378 PCOS prediction were, as expected, strong across the cohorts: 5.49, 10.9, and 17.1,  
379 respectively (**Supplementary Table 5**).

380

### 381 ***Clinical phenome analysis***

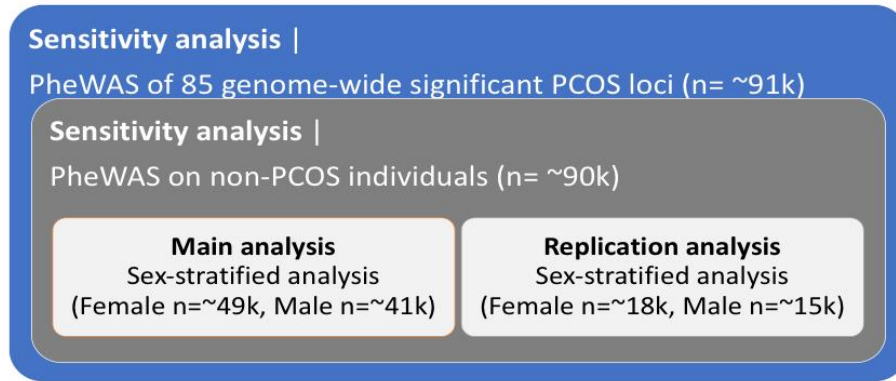
#### 382 ***A. Associated phenotypes with PRS (PheWAS-1)***

383 The general scheme of our PheWAS analyses are depicted in **Figure 5a**. Based on  
384 the model examination described above, the genome-wide PRS that includes all SNVs  
385 with p-value  $\leq 1$  was selected as the best performing PRS model and used for  
386 phenome-wide analysis. The phenomes of 49,343 female participants and 41,669 male  
387 participants were analyzed separately to test for association with high genetic risk for  
388 PCOS.

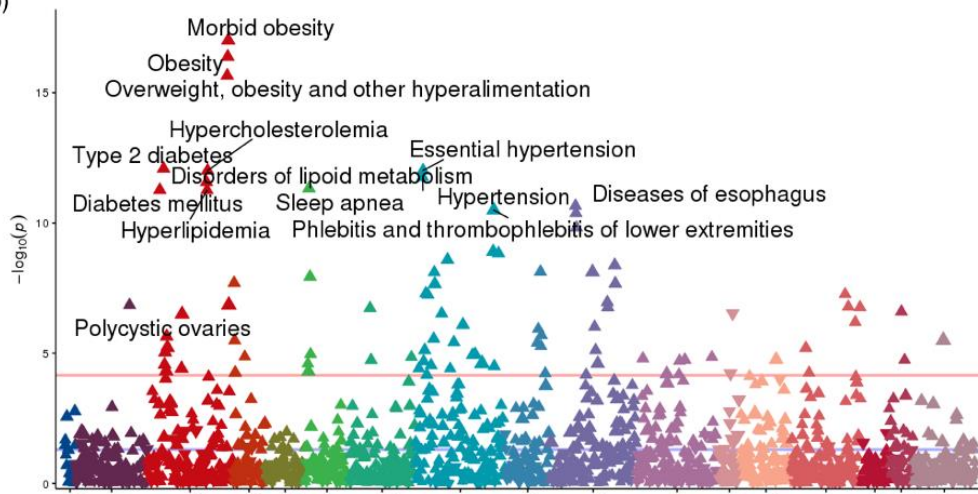
389 In the female PheWAS with PRS, 75 EHR phenotypes were identified with  
390 phenome wide significance (**Figure 5b, Supplementary Table 6a**). ‘Morbid obesity’  
391 (phecode 278.11) and obesity-related endocrine phenotypes, including ‘overweight,  
392 obesity, and other hyperalimentation’ (phecode 278), ‘type 2 diabetes’ (phecode 250.2),  
393 ‘essential hypertension’ (phecode 401.1) ‘hypercholesterolemia’ (phecode 272.11),  
394 ‘hypertension’ (phecode 401), ‘disorders of lipid metabolism’ (phecode 272) are the top-  
395 ranked. The phenome-wide significant association of ‘polycystic ovaries’ (phecode  
396 256.4) and PCOS-PRS are observed with one of the largest effect sizes (OR=1.015)  
397 among the result.

398 As a complex endocrine disorder, the PCOS pathophysiology seems to be tightly  
399 linked to the expression of endocrine or circulatory system manifestation. Among the 75

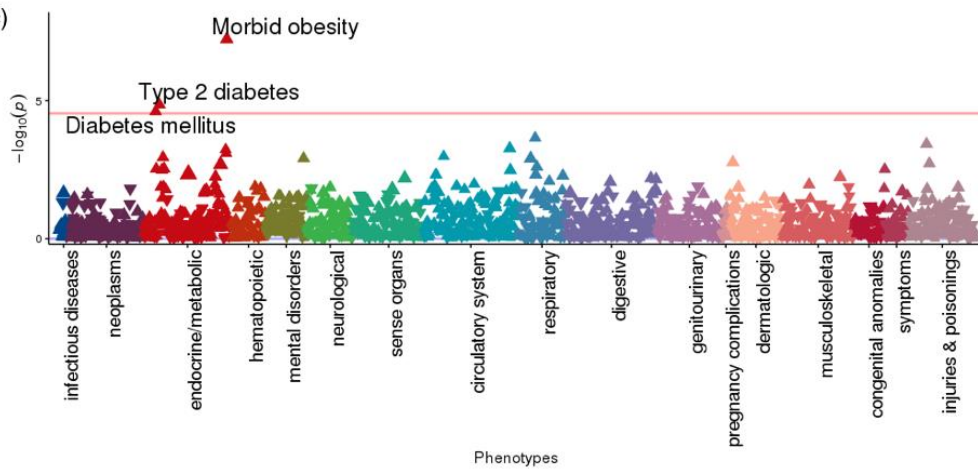
(a)



(b)



(c)



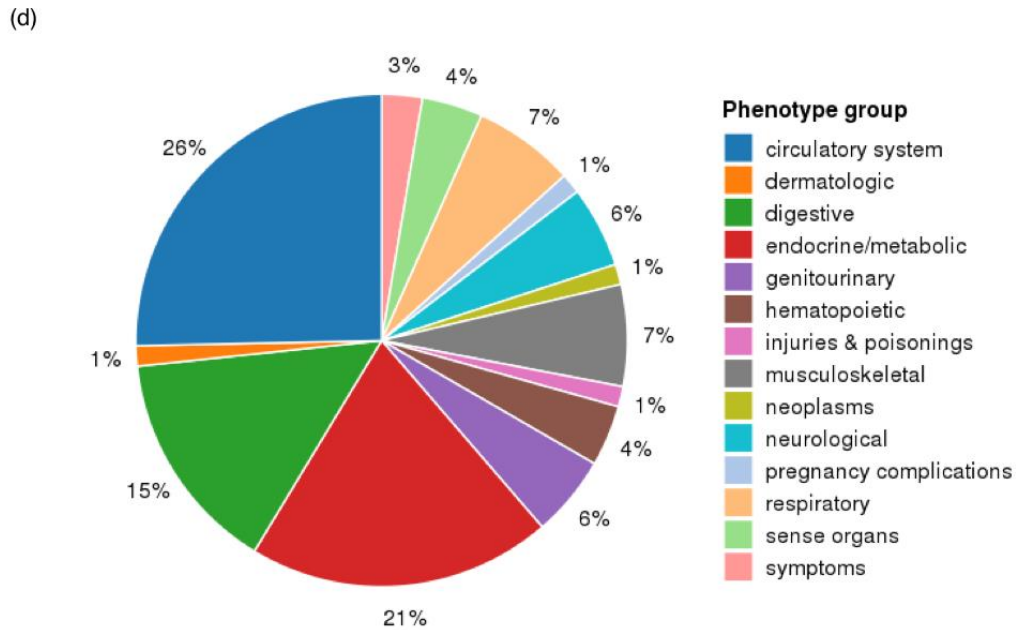


**Fig 5. PheWAS scheme and results using PRS.** (a) PheWAS scheme and sample sizes; (b) PheWAS Manhattan plot of PRS (SNVs with  $p$ -value  $\leq 1$ ); (c) PheWAS Manhattan plot of PRS (SNVs with  $p$ -value  $< 5E-08$ ); (d) pie chart summarizing PheWAS groups. In Manhattan plots (b) and (c), the x-axis represents the EHR phenotype categorical group and the y-axis represents the negative  $\log_{10}$  of the PheWAS  $p$ -value. Red lines indicate the cutoff for phenome-wide significance. For readability, only the most significant associations are annotated. Full lists of phenome-wide significant results are provided in Supplementary Tables 5 and 6, respectively. The pie chart in (d) shows EHR categories for the 72 phenome-wide significant phenotypes identified through PheWAS of the genome-wide PRS (SNVs with  $p$ -value  $\leq 1$ ).

400 phenome-wide significant traits with PRS, the phenotypes of circulatory system (26.0%)  
401 and endocrine/metabolic system (21.0%) appeared the most frequently (**Figure 5d**),  
402 while the four highest associated phenotypes are all endocrine/metabolic features.

403 Among the remainder of the phenome-wide significant phenotypes, associations of  
404 musculoskeletal phenotypes like ‘osteoarthritis’ (phecode 740 and 740.9) or ‘calcaneal  
405 spur; Exostosis NOS’ (phecode 726.4) possibly imply the hormonal changes on the  
406 skeletal system impacted by PCOS epidemiology. Multiple symptomatic genitourinary  
407 phenotypes of PCOS were also identified: ‘abnormal mammogram’ (phecode 611.1) or  
408 ‘other signs and symptoms in breast’ (phecode 613.7). An obesity-related pulmonary  
409 disorder of ‘sleep apnea’ (phecode 327.3) is also observed (classified as neurological  
410 phenotype in phecode map) with ‘obstructive sleep apnea’ (phecode 327.32). We could  
411 not identify any psychological or depression related phenotype that is known to have  
412 genetic correlation with the hormonal changes of PCOS.

413 The overall low range of OR (1.004~1.010) of the PheWAS results should be noted,  
414 which is assumedly due to the aggregated effects of the low impact SNVs for PCOS,  
415 especially in the full-inclusive PRS with the entire GWAS SNVs. The ORs from the  
416 generic PheWAS of individual PCOS SNVs are observed to be higher before merging  
417 them into the cumulative PRS, which is described later (**Supplementary Table 7**).

418 In the replication analysis on an independent cohort of 18,096 EA females (BioVU),  
419 16 out of 75 phenome-wide signals from the discovery analysis are replicated including  
420 ‘PCOS’ (p-value= $1.93 \times 10^{-2}$ , phecode 256.4) with the positive OR of 1.174 (**Table 5a**).  
421 Half of the replicated phenotypes (8 out of 16) belong to the endocrine/metabolic  
422 category. In particular, the following obesity-related endocrine phenotypes exhibit strong

**Table 5:** (a) 16 significant phenotypes of PRS (SNVs' p-value  $\leq 1$ ) female-stratified PheWAS that were phenome-wide significant in the discovery cohort (n=49,343) and successfully replicated in the independent VU cohort (n=18,096). (b) 3 phenome-wide significant results of PCOS-PRS (SNPs with  $P < 1$ ) male-stratified PheWAS from the discovery cohort (n=41,669) and replication cohort (n=15,612)

(a)			Discovery analysis					Replication analysis				
phecode	description	group	OR	SE	p	n_total	n_cases	OR	SE	p	n_total	n_cases
278.11	Morbid obesity	endocrine/metabolic	1.010	0.001	9.74E-18	37108	6790	1.116	0.029	1.64E-04	15329	1762
278.1	Obesity	endocrine/metabolic	1.008	0.001	4.14E-17	44267	13949	1.087	0.022	1.29E-04	17051	3484
278	Overweight, obesity and other hyperalimentation	endocrine/metabolic	1.007	0.001	2.20E-16	47803	17485	1.077	0.020	1.44E-04	18096	4529
250.2	Type 2 diabetes	endocrine/metabolic	1.007	0.001	8.18E-13	42874	10800	1.081	0.022	3.70E-04	16562	3660
327.3	Sleep apnea	neurological	1.008	0.001	4.71E-12	40673	6503	1.096	0.028	1.33E-03	15602	1847
250	Diabetes mellitus	endocrine/metabolic	1.007	0.001	5.39E-12	43325	11251	1.079	0.021	3.56E-04	16763	3861
571	Chronic liver disease and cirrhosis	digestive	1.008	0.001	4.17E-09	40531	4582	1.093	0.032	4.64E-03	15369	1463
539	Bariatric surgery	digestive	1.012	0.002	7.59E-09	47803	2034	1.202	0.055	8.00E-04	18096	439
327.32	Obstructive sleep apnea	neurological	1.007	0.001	1.16E-08	39291	5121	1.098	0.032	3.98E-03	15138	1383
571.5	Other chronic nonalcoholic liver disease	digestive	1.008	0.001	2.13E-08	40251	4302	1.112	0.033	1.38E-03	15219	1313
743.9	Osteopenia or other disorder of bone and cartilage	musculoskeletal	1.005	0.001	1.71E-07	43335	11354	0.956	0.022	4.45E-02	16019	3263
<b>256.4</b>	<b>Polycystic ovaries</b>	<b>endocrine/metabolic</b>	<b>1.015</b>	<b>0.003</b>	<b>3.16E-07</b>	<b>40696</b>	<b>942</b>	<b>1.174</b>	<b>0.069</b>	<b>1.93E-02</b>	<b>15637</b>	<b>281</b>
743	Osteoporosis, osteopenia and pathological fracture	musculoskeletal	1.004	0.001	6.38E-07	47803	15822	0.957	0.019	1.84E-02	18096	5340
250.3	Insulin pump user	endocrine/metabolic	1.008	0.002	2.25E-06	35057	2983	1.136	0.036	3.42E-04	14065	1163
250.23	Type 2 diabetes with ophthalmic manifestations	endocrine/metabolic	1.010	0.002	9.20E-06	33663	1589	1.221	0.062	1.20E-03	13272	370
627	Menopausal and postmenopausal disorders	genitourinary	1.004	0.001	1.40E-05	40468	14392	0.947	0.020	7.64E-03	16061	4301

(b)

phecode	description	group	Discovery analysis					Replication analysis				
			OR	SE	p	n_total	n_cases	OR	SE	p	n_total	n_cases
278.11	Morbid obesity	endocrine/metabolic	1.009	0.002	5.93E-08	32456	3489	1.049	0.036	1.78E-01	13465	1082
250.2	Type 2 diabetes	endocrine/metabolic	1.005	0.001	1.41E-05	36835	10984	1.031	0.021	1.49E-01	14000	4198
250	Diabetes mellitus	endocrine/metabolic	1.005	0.001	2.47E-05	37199	11348	1.029	0.021	1.70E-01	14180	4378

Phenome-wide significant threshold: p-value < 2.9E-5

423 evidence of replication after multiple testing correction (p-value <  $6.7 \times 10^{-5}$ , 0.05/75):  
424 ‘morbid obesity’ (phecode 278.11), ‘obesity’ (phecode 278.1), ‘overweight, obesity and  
425 other hyperalimentation’ (phecode 278). The well-known comorbidity between ‘type 2  
426 diabetes’ (phecode 250.2) and PCOS is also identified along with other diabetic  
427 syndromes like ‘diabetes mellitus’ (phecode 250). Other notable replicated phenotypes  
428 included multiple neurological and digestive manifestations, which have well-known  
429 association to obesity, such as ‘chronic liver disease and cirrhosis’ (phecode 571),  
430 ‘bariatric surgery’ (phecode 539) and ‘other chronic nonalcoholic liver disease’ (phecode  
431 571.5). An obesity-related pulmonary disorder of ‘sleep apnea’ (phecode 327.3) is also  
432 observed (classified as neurological phenotype in phecode map) with ‘obstructive sleep  
433 apnea’ (phecode 327.32).

434 In male-specific PheWAS with PRS (SNVs with p-value  $\leq 1$ ) model, three metabolic  
435 phenotypes reached phenome-wide significance in the discovery analysis: ‘morbid  
436 obesity’ (phecode 278.11), ‘type 2 diabetes’ (phecode 250.2), ‘diabetes mellitus’  
437 (phecode 250) which are known risk factors and/or co-morbidities for PCOS (**Figure 5b,**  
438 **Table 5b, Supplementary Table 6b**). However, none of the associations were  
439 replicated in the replication analysis on 15,611 independent males. It is possible that the  
440 replication sample remained underpowered and larger sample sizes will be needed to  
441 distinguish these results from a true null result.

442

#### 443 *B. Sensitivity analysis – Case-excluded analysis (PheWAS-2)*

444 After removing 949 PCOS patients in PheWAS investigation, we still identified 68  
445 PRS-phenotype associations that reached phenome-wide significance (**Supplementary**

446 **table 8)**, which is not very different from PheWAS-1. The result might be due to the  
447 challenge of current diagnosis practices in identifying PCOS cases, which implies the  
448 control groups are not completely excluding PCOS patients and possibly include some  
449 mixed signals from the unidentified PCOS cases. Alternatively, it is possible that genetic  
450 risk for PCOS remains a robust risk factor for these phenotypes even in the absence of  
451 clinical manifestations of PCOS.

452 The representative signals of diabetes/obesity-related endocrine traits that are  
453 identified in PheWAS-1 remained significant: ‘morbid obesity’ (phecode 278.11), ‘type 2  
454 diabetes’ (phecode 250.2), ‘obesity’ (phecode 278.1), ‘overweight, obesity and other  
455 hyperalimentation’ (phecode 278), ‘diabetes mellitus’ (phecode 250),  
456 ‘hypercholesterolemia’ (phecode 272.11), ‘disorders of lipid metabolism’ (phecode 272)  
457 and ‘hyperlipidemia’ (phecode 272.1) etc.

458 Four phenotypes no longer remained phenome-wide significant in PheWAS-2  
459 compared to PheWAS-1, including ‘menopausal and postmenopausal disorders’  
460 (phecode 627), ‘iron deficiency anemias, unspecified or not due to blood loss’ (phecode  
461 280.1), ‘sleep disorders’ (phecode 327) and ‘Insomnia’ (phecode 327.4). A new  
462 metabolic phenotype of ‘disorders of fluid, electrolyte, and acid-base balance’ (phecode  
463 276) was phenome-wide significance in PheWAS-2 compared to PheWAS-1, but the  
464 association did not remain significant in replication analysis. The phenome-wide  
465 significant phenotype with the largest effect size in PheWAS-2 is ‘localized adiposity’  
466 (OR=1.014, phecode 278.3), same as for PheWAS-1. It should be of note that the range  
467 of OR is low in PRS-PheWAS due to the cumulative effect sum of all PCOS  
468 susceptibility loci including low-effect variants.



469

470 *C. Sensitivity analysis – Associations with individual PCOS susceptibility loci*

471 **(PheWAS-3)**

472 In the individual PheWAS of 85 PCOS genome-wide significant variants, even  
473 though no association survives phenome-wide significance, likely due to the multiple  
474 testing burden, 11 PCOS variants show notable association to ‘polycystic ovaries’  
475 across the ancestry groups (Most significant variant hg19 chr11:30226528, OR=1.36,  
476 phecode 256.4), ranked as the second most significant phenotype (**Supplementary**  
477 **table 7**). Out of top 100 associations in PheWAS-3, the largest number of associations  
478 were related to circulatory system for ‘thrombotic microangiopathy’ (31.0%).  
479 Endocrine/metabolic related phenotypes were the second most frequent category  
480 (21.0%) composed of either ‘PCOS’ or ‘ovarian dysfunction’, and 12% of the top  
481 associations were digestive traits, largely devoted to diverticular diseases. We did not  
482 identify any associations related to obesity or diabetes, which were the most significant  
483 phenotypic features found in PheWAS-1 and PheWAS-2.

484

485 **Discussion**

486

487 A key question in precision medicine is how to identify patients at high risk for a  
488 given disease for the goal of targeting preventive care. In this study, we examined the  
489 ability of PRS to predict PCOS clinical diagnosis and mine comorbid EHR phenotypes  
490 with the ultimate goal of improving diagnostic accuracy for PCOS. We show that a PRS

491 for PCOS can be used (a) to identify patients at elevated risk of PCOS and (b) to  
492 determine the comorbid or pleiotropic phenome-wide expression associated with PCOS  
493 in a clinical setting.

494 The primary accomplishment of this study is a systematic enhancement of the  
495 polygenic risk prediction by integration of additional disease component phenotypes in  
496 the EHR into a PPRS. The onset of hirsutism, menstrual dysfunction, or female infertility  
497 are representative symptoms of PCOS and essential in determining clinical  
498 hyperandrogenism [10, 40, 41]. They are not required for a diagnosis of PCOS per se,  
499 but are useful in suggesting PCOS in a clinical context. The PPRS significantly  
500 improves the average explanatory power (pseudo- $R^2$ ) of PCOS prediction by 0.221  
501 (59.1-fold increase) compared to the null model without PRS or component phenotypes,  
502 and by 0.037 (14.7% increase) over the null model with the component phenotypes  
503 alone (**Table 2 and Figure 4**). In contrast to the previous studies that attempted to  
504 identify PCOS diagnosis with risk score calculation [13, 42], our algorithm did not limit  
505 risk predictor in a single-dimension, using both phenotype and genotype markers with  
506 polygenic inheritance, and extensively demonstrated the predictive performance of  
507 PPRS with several machine-learning techniques. The findings shown here strengthen  
508 the potential clinical utility of PPRS as a disease predictor, particularly when combined  
509 with component symptom information available within the EHR.

510 To date, research has consistently shown that the PRS built from EA GWAS data  
511 does not perform as robustly across non-EA samples. In this study, we assessed the  
512 performance of a Eurocentrically built PCOS-PRS on the samples of EA, AA, and the  
513 joint MA cohorts. Undeniably, validation statistics varied by ancestry group and the

514 PCOS diagnosis prediction in AA cohort shows the poorest performance. However, it is  
515 of note that more than half of the tested models in AA still show statistical significance in  
516 terms of regression p-value, and those models display a reliable efficiency for PCOS  
517 detection in effect size and AUC (**Table 3**). Interestingly, the ORs for PRS differ across  
518 the ancestry cohorts, and somewhat higher in some prediction models in AA (average  
519 OR of model1=1.25, model2=1.28) and MA samples (average OR of model1=1.14,  
520 model2=1.13) than EA samples (average OR of model1=1.13, model2=1.12). The  
521 overall ORs of the PRS variable are fairly stable throughout all polygenic prediction  
522 models (OR 1.12~1.28). The observed significance of the PRS variable in the MA  
523 cohort, more stable than in the EA or AA participants alone, is likely due to the  
524 increased statistical power with larger sample size that counters the sample  
525 heterogeneity introduced. In addition, we found that the accumulation of genetic variants  
526 did not always increase the predictive capability of PRS in terms of pseudo-R<sup>2</sup> and OR  
527 (**Figure 3, Table 2**). This might be due to the different RAF of PCOS risk variants by  
528 different PRS p-value cutoffs, and the varying LD structure of the ancestry groups.  
529 Previous research has confirmed that the LD pattern varies between EA and Chinese  
530 women at the PCOS susceptibility loci encoding LH/choriogonadotropin receptor  
531 (*LHCGR*) and FSH receptor (*FSHR*) genes, but the reproducible signals of the loci are  
532 consistently associated to PCOS regardless of ancestry[43, 44]. Our sensitivity analysis  
533 (PheWAS-3) also suggests the varying phenotypic effect of PCOS loci in different  
534 ancestries, but confirms the strong association with PCOS nonetheless. These findings  
535 demonstrate the primary role of PCOS-PRS in cumulatively explaining substantial

536 variation of disease susceptibility across ancestries even with differing LD structures,  
537 and extend the general utility of PPRS in disease prediction.

538 Furthermore, our PRS-based phenome-wide analysis revealed several clinical  
539 associations that are tightly linked with obesity, confirming the shared metabolic  
540 pathways between PCOS and obesity in a phenomic aspect. As obesity is a common  
541 finding which can be found in 50-65% of PCOS patients[10], and previous Mendelian  
542 randomization study revealed the causal relationship of BMI on PCOS etiology[45],  
543 many of our findings could be interpreted as phenotypic evidence of co-morbid obesity.  
544 'Morbid obesity' (phecode 278.11), 'hypercholesterolemia' (phecode 272.11), 'disorders  
545 of lipid metabolism' (phecode 272), 'hyperlipidemia' (phecode 272.1), 'hypertension'  
546 (phecode 401) or 'abnormal glucose' (phecode 250.4) are easily understandable with  
547 the context of heightened metabolic risks for obesity. 'Sleep apnea' (phecode 327.3)  
548 and 'chronic liver disease and cirrhosis' (phecode 571), 'GERD' (phecode 530.11),  
549 'diseases of esophagus' (phecode 530 and 530.1) are either neurological, pulmonary or  
550 digestive assorted symptoms that are commonly found in the patients with obesity.

551 It is also noteworthy that there were 75 significant associations identified in women  
552 while in men, there were only three significantly associated diagnosis (morbid obesity,  
553 type 2 diabetes, diabetes mellitus) despite a similar sample size for males and females  
554 in the analysis. It is possible that the clinical consequences of high androgens in males  
555 are less likely to cause symptoms for which medical treatment is sought, or that these  
556 genetic variants only elevate androgen levels in a female 'environment' but not a male  
557 one. The three identified phenotypes in males additionally suggest that if an individual

558 harbors high genetic risk for PCOS, the metabolic manifestations are similar regardless  
559 of sex.

560 Consistent with previous studies [13, 45], we identified phenotypic evidence of  
561 positive BMI association with genetic risk of PCOS. In the stratification analysis of PRS,  
562 our observation of the increased BMI in individuals with high risk of PCOS are evident in  
563 both EA and MA cohorts (**Figure 2**). The comorbid phenotypes could be driven by  
564 pleiotropy in which PCOS-associated genes also increase BMI, or could be due to  
565 under diagnosis of PCOS itself, in which case the association with obesity phenotypes  
566 may be a result of comorbidity with undiagnosed PCOS.

567 Several limitations to this study need to be acknowledged. First, the sample size of  
568 AA participants was relatively small which increases the likelihood of both false negative  
569 and false positive findings. Further investigation is needed to fully understand the  
570 overlap in PCOS genetic factors across multi-ancestry participants and the  
571 methodological application of Eurocentric PCOS-PRS to other genetic ancestries  
572 considering LD structure. Secondly, the phenotypic components we used for polygenic  
573 prediction are currently limited to only three representative phenotypes: hirsutism,  
574 irregular menstruation, and female infertility. Fueled by our PheWAS finding, the work  
575 could be extended by incorporating the additional phenotypes that might increase the  
576 likelihood of an eventual diagnosis. Also, the phecode of PCOS used for PheWAS was  
577 converted from ICD-9-CM 256.4 and ICD-10-CM E28.2, which was used as a proxy for  
578 capturing PCOS in the EMR. This phecode may not perfectly capture PCOS as they  
579 may or may not capture hyperandrogenemia. The selection bias in our discovery cohort  
580 should be acknowledged as well. Two of our participating sites (Geisinger and

581 Marshfield) mainly recruited their patients for the study of obesity and type 2 diabetes,  
582 which resulted in a higher proportion of obese patients into their biobank and therefore  
583 may inflate the prevalence of PCOS in these subgroups. Lastly, due to the low  
584 diagnosis rate of PCOS patients in current EHR system, it is possible that unidentified  
585 PCOS cases could reduce power in each analysis.

586 Our approach has provided a novel methodological opportunity to stratify patients'  
587 genetic risk and to discover the phenomic network associated with PCOS pathogenesis.  
588 Integrative analysis of the PRS-PheWAS enables the systematic interrogation of PCOS  
589 comorbidity patterns across the phenome, which cannot be readily identified by a  
590 single-variant approach. The identified phenomic networks could be used at the stage of  
591 first screening, prior to the testing of hormones or imaging of ovaries, or to help the  
592 patient and physician decide whether more extensive testing would be useful for PCOS  
593 diagnosis. From a precision medicine perspective, such an approach may provide a  
594 greater understanding of a patient's clinical presentation and suspected diagnosis  
595 based on phenotypic or genetic variations.

596

## Reference

1. Davies N. PCOS: Polycystic Ovarian Syndrome. *Diabetes Self Manag.* 2016;33(1):44-7.
2. Azziz R, Marin C, Hoq L, Badamgarav E, Song P. Health care-related economic burden of the polycystic ovary syndrome during the reproductive life span. *J Clin Endocrinol Metab.* 2005;90(8):4650-8.
3. Society TE. *Endocrine Facts and Figures: Reproduction and Development.* 2017.
4. Yawn V. Polycystic ovarian syndrome. *Adv NPs PAs.* 2012;3(12):11-4; quiz 5.
5. Vink JM, Sadzadeh S, Lambalk CB, Boomsma DI. Heritability of polycystic ovary syndrome in a Dutch twin-family study. *J Clin Endocrinol Metab.* 2006;91(6):2100-4.
6. Jahanfar S, Eden JA, Nguyen T, Wang XL, Wilcken DE. A twin study of polycystic ovary syndrome and lipids. *Gynecol Endocrinol.* 1997;11(2):111-7.
7. Jahanfar S, Eden JA, Warren P, Seppala M, Nguyen TV. A twin study of polycystic ovary syndrome. *Fertil Steril.* 1995;63(3):478-86.
8. Broekmans FJ, Knauff EA, Valkenburg O, Laven JS, Eijkemans MJ, Fauser BC. PCOS according to the Rotterdam consensus criteria: Change in prevalence among WHO-II anovulation and association with metabolic factors. *BJOG.* 2006;113(10):1210-7.
9. Li L, Baek KH. Molecular genetics of polycystic ovary syndrome: an update. *Curr Mol Med.* 2015;15(4):331-42.
10. Futterweit W. Polycystic ovary syndrome: clinical perspectives and management. *Obstet Gynecol Surv.* 1999;54(6):403-13.
11. Wolf WM, Wattick RA, Kinkade ON, Olfert MD. Geographical Prevalence of Polycystic Ovary Syndrome as Determined by Region and Race/Ethnicity. *Int J Env Res Pub He.* 2018;15(11).
12. Carmina E. Diagnosis of polycystic ovary syndrome: from NIH criteria to ESHRE-ASRM guidelines. *Minerva Ginecol.* 2004;56(1):1-6.
13. Day F, Karaderi T, Jones MR, Meun C, He C, Drong A, et al. Large-scale genome-wide meta-analysis of polycystic ovary syndrome suggests shared genetic architecture for different diagnosis criteria. *PLoS Genet.* 2018;14(12):e1007813.
14. Dewailly D. Diagnostic criteria for PCOS: Is there a need for a rethink? *Best Pract Res Clin Obstet Gynaecol.* 2016;37:5-11.
15. Agapova SE, Cameo T, Sopher AB, Oberfield SE. Diagnosis and challenges of polycystic ovary syndrome in adolescence. *Semin Reprod Med.* 2014;32(3):194-201.
16. Fritsche LG, Gruber SB, Wu Z, Schmidt EM, Zawistowski M, Moser SE, et al. Association of Polygenic Risk Scores for Multiple Cancers in a Phenome-wide Study: Results from The Michigan Genomics Initiative. *Am J Hum Genet.* 2018;102(6):1048-61.
17. International Schizophrenia C, Purcell SM, Wray NR, Stone JL, Visscher PM, O'Donovan MC, et al. Common polygenic variation contributes to risk of schizophrenia and bipolar disorder. *Nature.* 2009;460(7256):748-52.



18. Khera AV, Chaffin M, Aragam KG, Haas ME, Roselli C, Choi SH, et al. Genome-wide polygenic scores for common diseases identify individuals with risk equivalent to monogenic mutations. *Nat Genet.* 2018;50(9):1219-24.
19. Zheutlin AB, Dennis J, Restrepo N, Straub P, Ruderfer D, Castro VM, et al. Penetrance and pleiotropy of polygenic risk scores for schizophrenia in 90,000 patients across three healthcare systems. *bioRxiv.* 2018:421164.
20. Carroll RJ, Bastarache L, Denny JC. R PheWAS: data analysis and plotting tools for phenome-wide association studies in the R environment. *Bioinformatics.* 2014;30(16):2375-6.
21. Denny JC, Ritchie MD, Basford MA, Pulley JM, Bastarache L, Brown-Gentry K, et al. PheWAS: demonstrating the feasibility of a phenome-wide scan to discover gene-disease associations. *Bioinformatics.* 2010;26(9):1205-10.
22. Martin AR, Kanai M, Kamatani Y, Okada Y, Neale BM, Daly MJ. Hidden 'risk' in polygenic scores: clinical use today could exacerbate health disparities. *bioRxiv.* 2019:441261.
23. Rosenberg NA, Edge MD, Pritchard JK, Feldman MW. Interpreting polygenic scores, polygenic adaptation, and human phenotypic differences. *Evolution, Medicine, and Public Health.* 2018:eoy036-eoy.
24. Duncan L, Shen H, Gelaye B, Ressler K, Feldman M, Peterson R, et al. Analysis of Polygenic Score Usage and Performance in Diverse Human Populations. *bioRxiv.* 2018:398396.
25. Martin AR, Kanai M, Kamatani Y, Okada Y, Neale BM, Daly MJ. Hidden 'risk' in polygenic scores: clinical use today could exacerbate health disparities. *bioRxiv.* 2018:441261.
26. Martin AR, Gignoux CR, Walters RK, Wojcik GL, Neale BM, Gravel S, et al. Human Demographic History Impacts Genetic Risk Prediction across Diverse Populations. *Am J Hum Genet.* 2017;100(4):635-49.
27. Curtis D. Polygenic risk score for schizophrenia is more strongly associated with ancestry than with schizophrenia. *bioRxiv.* 2018:287136.
28. McCarty CA, Chisholm RL, Chute CG, Kullo IJ, Jarvik GP, Larson EB, et al. The eMERGE Network: a consortium of biorepositories linked to electronic medical records data for conducting genomic studies. *BMC Med Genomics.* 2011;4:13.
29. Stanaway IB, Hall TO, Rosenthal EA, Palmer M, Naranbhai V, Knevel R, et al. The eMERGE genotype set of 83,717 subjects imputed to ~40 million variants genome wide and association with the herpes zoster medical record phenotype. *Genet Epidemiol.* 2019;43(1):63-81.
30. Kho AN, Pacheco JA, Peissig PL, Rasmussen L, Newton KM, Weston N, et al. Electronic medical records for genetic research: results of the eMERGE consortium. *Sci Transl Med.* 2011;3(79):79re1.
31. Purcell S, Neale B, Todd-Brown K, Thomas L, Ferreira MA, Bender D, et al. PLINK: a tool set for whole-genome association and population-based linkage analyses. *Am J Hum Genet.* 2007;81(3):559-75.
32. Euesden J, Lewis CM, O'Reilly PF. PRSice: Polygenic Risk Score software. *Bioinformatics.* 2015;31(9):1466-8.



33. Denny JC, Bastarache L, Ritchie MD, Carroll RJ, Zink R, Mosley JD, et al. Systematic comparison of phenome-wide association study of electronic medical record data and genome-wide association study data. *Nat Biotechnol.* 2013;31(12):1102-10.
34. Wu P, Gifford A, Meng X, Li X, Campbell H, Varley T, et al. Developing and Evaluating Mappings of ICD-10 and ICD-10-CM codes to Phecodes. *bioRxiv.* 2018:462077.
35. Das S, Forer L, Schonherr S, Sidore C, Locke AE, Kwong A, et al. Next-generation genotype imputation service and methods. *Nat Genet.* 2016;48(10):1284-7.
36. McCarthy S, Das S, Kretzschmar W, Delaneau O, Wood AR, Teumer A, et al. A reference panel of 64,976 haplotypes for genotype imputation. *Nat Genet.* 2016;48(10):1279-83.
37. McFadden D. Conditional logit analysis of qualitative choice behavior. *Frontiers in Econometrics.* 1973:105-42.
38. Plomin R, Haworth CM, Davis OS. Common disorders are quantitative traits. *Nat Rev Genet.* 2009;10(12):872-8.
39. Krapohl E, Euesden J, Zabaneh D, Pingault JB, Rimfeld K, von Stumm S, et al. Phenome-wide analysis of genome-wide polygenic scores. *Mol Psychiatry.* 2016;21(9):1188-93.
40. Goodman NF, Cobin RH, Futterweit W, Glueck JS, Legro RS, Carmina E, et al. American Association of Clinical Endocrinologists, American College of Endocrinology, and Androgen Excess and Pcos Society Disease State Clinical Review: Guide to the Best Practices in the Evaluation and Treatment of Polycystic Ovary Syndrome--Part 1. *Endocr Pract.* 2015;21(11):1291-300.
41. Rosenfield RL, Lucky AW. Acne, hirsutism, and alopecia in adolescent girls. Clinical expressions of androgen excess. *Endocrinol Metab Clin North Am.* 1993;22(3):507-32.
42. Deshmukh H, Papageorgiou M, Kilpatrick ES, Atkin SL, Sathyapalan T. Development of a novel risk prediction and risk stratification score for polycystic ovary syndrome. *Clin Endocrinol (Oxf).* 2019;90(1):162-9.
43. Mutharasan P, Galdones E, Penalver Bernabe B, Garcia OA, Jafari N, Shea LD, et al. Evidence for chromosome 2p16.3 polycystic ovary syndrome susceptibility locus in affected women of European ancestry. *J Clin Endocrinol Metab.* 2013;98(1):E185-90.
44. Chen ZJ, Zhao H, He L, Shi Y, Qin Y, Shi Y, et al. Genome-wide association study identifies susceptibility loci for polycystic ovary syndrome on chromosome 2p16.3, 2p21 and 9q33.3. *Nat Genet.* 2011;43(1):55-9.
45. Day FR, Hinds DA, Tung JY, Stolk L, Styrkarsdottir U, Saxena R, et al. Causal mechanisms and balancing selection inferred from genetic associations with polycystic ovary syndrome. *Nat Commun.* 2015;6:8464.

## **Acknowledgements**

The phase III of the eMERGE Network was initiated and funded by the NHGRI through the following grants: U01HG008657 (Kaiser Permanente Washington/University of Washington School of Medicine); U01HG008685 (Brigham and Women's Hospital); U01HG008672 (Vanderbilt University Medical Center); U01HG008666 (Cincinnati Children's Hospital Medical Center); U01HG006379 (Mayo Clinic); U01HG008679 (Geisinger Clinic); U01HG008680 (Columbia University Health Sciences); U01HG008684 (Children's Hospital of Philadelphia); U01HG008673 (Northwestern University); U01HG008701 (Vanderbilt University Medical Center serving as the Coordinating Center); U01HG008676 (Partners Healthcare/Broad Institute); and U01HG008664 (Baylor College of Medicine).

## **The International PCOS Consortium members**

Felix Day, Tugce Karaderi, Michelle R. Jones, Cindy Meun, Chunyan He, Alex Drong, Peter Kraft, Nan Lin, Hongyan Huang, Linda Broer, Reedik Magi, Richa Saxena, Triin Laisk-Podar, Margrit Urbanek, M. Geoffrey Hayes, Gudmar Thorleifsson, Juan Fernandez-Tajes, Anubha Mahajan, Benjamin H. Mullin, Bronwyn G.A. Stuckey, Timothy D. Spector, Scott G. Wilson, Mark O. Goodarzi, Lea Davis, Barbara Obermeyer-Pietsch, André G. Uitterlinden, Verner Anttila, Benjamin M Neale, Marjo-Riitta Jarvelin, Bart Fauser, Irina Kowalska, Jenny A. Visser, Marianne Anderson, Ken Ong, Elisabet Stener-Victorin, David Ehrmann, Richard S. Legro, Andres Salumets, Mark I. McCarthy, Laure Morin-Papunen, Unnur Thorsteinsdottir, Kari Stefansson,

Unnur Styrkarsdottir, John Perry, Andrea Dunaif, Joop Laven, Steve Franks, Cecilia M. Lindgren, Corrine K. Welt

### **Authors' contributions**

YYJ, LD and MGH designed the study; IBS and DRC imputed and quality controlled the genotype array data missing variants with input from GPJ; JAP, AOB, RC, DRC, JCD, DRVE, HH, JBH, SJH, KH, GPJ, FDM, SP, MDR, IBS contributed to eMERGE genotype and phenotype data generation; LD, MGH, FD, MJ, TK, CM generated PCOS GWAS data through the International PCOS consortium; YYJ performed statistical analysis in discovery cohort and validated the algorithms; KA performed statistical analysis in replication cohort; YYJ, ANK, LD and MGH interpreted the results; YYJ, KA, JAP, ANK, LD, MGH drafted the manuscript; YYJ designed the figures and created the tables; All authors critically reviewed the manuscript for important intellectual content; DRC, GPJ, MS and RLC obtained the funding.

### **Competing interest statement**

The authors report no competing interests.